THE EFFECT OF FeO ACTIVITY ON THE MATERIAL AND ENERGY FLOW IN A NOVEL SUSPENSION IRONMAKING PROCESS

by

Shuhua Liu

A thesis submitted to the faculty of
The University of Utah
in partial fulfillment of the requirements for the degree of

Master of Science

Department of Metallurgical Engineering

The University of Utah

December 2011

The University of Utah Graduate School

STATEMENT OF THESIS APPROVAL

The thesis of **Shuhua Liu**

has been approved by the following supervisory committee members:

Hong Yong Sohn	, Chair	**May 09, 2011** Date Approved
Michael S. Moats	, Member	**May 09, 2011** Date Approved
Hang Goo Kim	, Member	**May 09, 2011** Date Approved

and by **Jan D. Miller** , Chair of

the Department of **Metallurgical Engineering**

and by Charles A. Wight, Dean of The Graduate School.

ABSTRACT

A one-million ton hot iron per year suspension ironmaking plant has been simulated with the consideration of activity coefficient of FeO in slag by using Metsim simulation software package for calculating material balance and energy balance in this thesis. Mathematical models found in the literature for calculating the activity coefficient of FeO in slag were first selected, reviewed and assessed. Park and Lee's regular solution model was evaluated to be the most appropriate model for this study, and was integrated with the Metsim simulation software for the simulation of the suspension ironmaking process.

Six suspension ironmaking processes were simulated: one-step process with pure H_2, two-step process with pure H_2, one-step reformerless process with natural gas, two-step reformerless process with natural gas, one-step process with SMR-H_2 and one-step process with SMR-syngas. The simulated results show that the suspension ironmaking processes with pure H_2 and reformerless natural gas are more energy efficient than conventional blast furnace ironmaking process, mainly due to the direct use of iron ore concentrate and no need for coke in the suspension ironmaking processes. The reformerless suspension ironmaking process with natural gas would consume 30 – 41% less energy than the average blast furnace ironmaking process.

On the basis of material balance and energy balance, the economical feasibility of the suspension ironmaking process was analyzed. Capital cost, operating cost, CO_2

credit and net present value were used in analyzing economic feasibility of the suspension ironmaking process.

The analyzed results show that pure H_2 process would require the least capital cost and receive the largest CO_2 credit, but need the highest operating cost. Even without considering CO_2 credit, except pure H_2 process, all other suspension ironmaking processes would be profitable with positive NPV values. With sufficient CO_2 credit, all suspension ironmaking processes simulated would be profitable, among which reformerless natural gas would return the best economics.

Capital cost for the one-million ton per year suspension ironmakng plant with reformerless natural gas would be $414 million for one-step and $537 million for two-step, operating cost $429/tHI and $418/tHI, and NPV $333/tHI and $177/tHI without CO_2 credit and $813/tHI and $795/tHI with $100/t CO_2 credit, respectively.

Economic sensitivity was also analyzed. Lower fuel price, lower operating cost, higher hot iron price and larger CO_2 credit would all help improve the economics of the suspension ironmaking process.

TABLE OF CONTENTS

LIST OF TABLES

LIST OF FIGURES

LIST OF SYMBOLES

1st	one-step
2st	two-step
α_i	activity of component i
β	iron reduction rate
γ_i	activity coefficient of component i
k	reaction equilibrium constant
p_i	partial pressure of component i
ΔG^o	Gibbs free energy change
BF	Blast Furnace
BFW	Boiler Feed Water
DF	Driving Force
N_{gas}	Natural gas
NPV	Net Present Value
tHI	ton of Hot Iron
PSA	Pressure Swing Adaptor
SMR	Steam Methane Reforming
WGS	Water Gas Shift
WHB	Waste Heat Boiler
SRMSSD	Square Root of Mean Sum of Squares of Differences

ACKNOWLEDGEMENTS

I am heartily thankful to my thesis advisor, Professor H.Y. Sohn, for his invaluable guidance and advice.

I would also like to express my sincerest gratitude to Professor H. G. Kim and Professor M. S. Moats for their wonderful instruction.

My special thanks go to my father Zhiping Liu and my mother Yunfang Wang for their unselfish love and unlimited care. I would like to express my deepest appreciation to my husband, Naiyang Ma, my daughter, Rui Ma and my son, Richard Xianxiang Ma, for their understanding, support and love.

Our family friend Ms. Mildred Yvonne Smith deserves my special thanks for her precious friendship and love.

I would like to express my gratitude to my project research colleague, Haruka Kimura Pinegar, whose invaluable help and support enabled me to complete my research. It was my pleasure to work with my fellow colleagues, Haitao Wang, Yousef Mohassab, Moo Eob Choi, Liangzhu Zhu, M. Olivas-Martinez, Xu Wang and Jun Gao. Their help and friendship are highly appreciated.

This work was supported by the American Iron and Steel Institute (AISI) with respect to its Technology Roadmap Program under Cooperative Agreement No. DE-FC36-97ID13554 with the US Department of Energy and a further research service Agreement between AISI and the University of Utah under AISI's CO_2 Breakthrough Program.

CHAPTER 1

INTRODUCTION

1.1. Existing Ironmaking Technologies

Steel is one of humankind's greatest inventions. It is widely used in modern society. Due to economic growth and population increase, the world will continue to demand more steel, especially in Asia and other emerging areas.

At present, two kinds of steelmaking processes dominate the steel industry, conventional integrated steelmaking using blast furnaces (BF) and basic oxygen furnaces (BOF), and mini steelmaking using electric arc furnaces (EAF). Globally, the integrated steelmaking process produces around 60% of steel and the remaining 40% of steel is made by the mini steelmaking process [1]. In the integrated steelmaking process, BF utilizes iron ore, coke and flux to produce hot iron for BOF to produce steel, while in the mini steelmaking process, steel scrap is used to make steel. Constrained by the limited amount of steel scrap in the world market, the mini steelmaking, EAF process can supply only a limited amount of the steel the world demands. As a result, in the foreseeable future, the conventional integrated steelmaking, BF-BOF process will continue to play a significant role in steel production. An ironmaking blast furnace is a shaft furnace reactor in which ironmaking is a countercurrent process. Solid raw materials (sinter, pellets, lump iron ore, coke and flux as needed) are charged from the top of the furnace. High -

temperature hot air is blown through tuyeres in the furnace. Supplementary fuels, such as pulverized coal, natural gas and oil, can also be injected into the furnace through the tuyeres. The hot air reacts with coke and injected fuels, forming 2,000 – 2,500 °C hot gas. This hot gas rises and passes through raw materials that are descending from the top to the bottom of the furnace. In the process when the hot gas is ascending, it transfers its heat to the raw materials and its temperature decreases, while the raw materials receive heat from the hot gas and experience a series of physiochemical changes. Iron oxides in the raw materials are reduced by CO and H_2 in the gas and solid carbon in coke. The raw materials gradually soften and melt. Liquid hot iron and molten slag are formed in the hearth of the furnace.

Even though BF ironmaking itself is a very efficient process[1], the use of metallurgical coke has prevented/limited its development because world reserves of coking coal are limited and not uniformly distributed. This requirement of metallurgical coke makes BF ironmaking more and more expensive. Besides, along with cokemaking, preparation of iron ores for blast furnaces, such as making sinter and pellets, often results in high energy consumption, heavy environmental pollution and large CO_2 footprints. For these reasons, it was predicted that BF ironmaking would fall to 60% in 2050 [1] from around 90% of the current total iron production.

As an alternative, direct reduced iron (DRI) has increased significantly in recent years. There are two kinds of DRI processes. One is gas-based, such as MIDREX and HYL/Energiron, and the other is coal-based, such as rotary kiln process and fluidized bed FINMET process. These DRI processes, however, have several problems. For example, kilns need high-reactivity coal with a high melting temperature of ash [2], and

gas-based DRI processes need high-grade iron ores. These special requirements often cause higher DRI cost than scrap [2]. Some other problems in DRI processes include high refractory consumption, particle sticking/fusion [3], requirement of lump ore or agglomerated iron ores, and difficulties in handling DRI product due to its high reactivity.[4] As a result, DRI production has not been high enough to replace blast furnaces to a significant extent.

Smelting reduction is another recent alternative to BF ironmaking. It uses coal, instead of coke, as a reducing agent and fuel. However, not all smelting reduction processes directly use iron ore concentrate, and have lower energy requirements and lower CO_2 emissions than BF [5-6]. Corex and FINEX processes are examples of smelting reduction ironmaking processes. There are several other disadvantages about smelting reduction process, such as high FeO in slag, severe lining corrosion. [2].

1.2. Suspension Ironmaking Technology

In order to solve the problems of existing ironmaking processes and to improve the global environment, "gas-solid suspension ironmaking technology" has been proposed and developed as an energy-saving and environment-friendly ironmaking process by Sohn [7] at the University of Utah. This process, which has been confirmed in small-scale lab tests and is currently undergoing large laboratory-scale testing, can produce iron by directly using iron ore concentrate with gaseous reductants such as hydrogen, natural gas, syngas, or a combination thereof. [7-11] Compared to other gas-based ironmaking processes, the suspension ironmaking process has several advantages.

First, the suspension ironmaking process directly uses iron ore concentrate, which is

produced in the U.S. and elsewhere in large quantities. Therefore, this process can avoid the problems that the existing ironmaking technologies are facing, such as high energy consumption and heavy environmental pollution in sintering, pelletization and cokemaking. Other problems, such as particle fusion, sticking or disintegration of pellets, can also be avoided.

Second, suspension ironmaking technology provides a possibility for making steel from iron ore concentrate in a single continuous process [7]. Especially, if hydrogen is used as a reductant, hot iron will not contain carbon and can be directly sent to refining or alloying steps.

In addition, since hydrogen can reduce iron oxide at a much faster rate, this presents the highest potential for a high-intensity ironmaking technology [7-11]. Bench scale experiments of suspension reduction using hydrogen have shown that the reduction rate of iron ore concentrate is sufficiently high at 1200^{o}C or higher temperatures under excess hydrogen to overcome the equilibrium of the reduction of wustite by hydrogen [7-11]. Material and energy balance calculations previously performed indicated that the proposed process using hydrogen would consume 38% less energy and emit only 4% of carbon dioxide compared to the current blast furnace operation [7-11]. From these perspectives, the proposed suspension ironmaking process is expected to have considerable energy and environmental benefits.

1.3. Previous Work on Simulation of the Suspension Ironmaking Process

Pinegar (formerly Kimura) et al.[12], using the Metsim simulation software package, first conducted simulation of one-step and two-step suspension ironmaking

process with pure H_2. In that simulation, operating temperature, preheating temperature and hydrogen driving force were considered and examined.

Based on the simulation framework of suspension ironmaking process with pure H_2, Pinegar et al.[13-14] developed simulation frameworks for one-step and two-step reformerless suspension ironmaking process with natural gas, SMR-H_2 and SMR-syngas. Besides the Metsim simulation, Pinegar also made use of the results of material balance and energy balance, and conducted analysis of economical feasibility for the suspension ironmaking process with different H_2 sources[15-16].

In the previous simulation study of suspension ironmaking process, 99% reduction ratio of iron in iron ore concentrate was assumed in the process [12-14, 17], and FeO activity in slag was not considered.

1.4. Role of FeO Activity Coefficient in Calculation of Material Balance and Energy Balance of the Suspension Ironmaking Process

As stated above, previous work of process simulation was based on an assumption of 99% Fe reduction ratio. As the first step of the process simulation, this assumption was necessary to reduce the complexity of the calculation. However, after the general picture of the process material balance and energy balance has been displayed, it is of importance to examine the effects of this assumption. Furthermore, with the well-built foundation of previous work of process simulation, more variables should be included, tested and simulated, so that the process can be understood with more detail.

In the suspension ironmaking process, the reduction of wustite into iron is a key step. The reaction can be expressed by

$$FeO_{(S)} + H_{2(g)} = Fe_{(l)} + H_2O_{(g)}. \quad (1.1)$$

Equilibrium constant k of reaction (1.1) can be calculated by

$$k = \frac{P_{H_2O}}{P_{H_2}} \frac{a_{Fe}}{a_{FeO}} \quad (1.2)$$

where, p_{H2O} and p_{H2} are equilibrium partial pressures of H_2O and H_2 in the gas, and a_{Fe} and a_{FeO} are the activities of iron in hot iron and FeO in slag, respectively. Obviously, a_{Fe}=1 and $a_{FeO} = \gamma_{FeO} X_{FeO}$. Here, γ_{FeO} and X_{FeO} are activity coefficient and mole fraction of FeO in slag. Then, Eq. (1.2) turns to

$$k = \frac{P_{H_2O}}{P_{H_2}} \frac{1}{\gamma_{FeO} X_{FeO}}. \quad (1.3)$$

According to the relationship between equilibrium constant k and standard Gibbs free energy change ΔG^0, equilibrium mole fraction of FeO in slag can be calculated by

$$X_{FeO} = \frac{P_{H_2O}}{P_{H_2}} \frac{1}{\gamma_{FeO}} e^{\Delta G^0 / RT}, \quad (1.4)$$

where T is reaction temperature and R is the gas constant.

The reduction ratio of iron, β, in the process is defined as ratio of reduced iron to total iron. Assume slag ratio is S kg/tFe. Then Fe reduction ratio β is

$$\beta = \frac{1000}{1000 + SCX_{FeO}}. \quad (1.5)$$

C in Eq. (1.5) is a conversion factor of mole fraction of FeO to weight percentage of Fe in slag. Substitute Eq. (1.4) into Eq. (1.5)

$$\beta = \frac{1000}{1000+SC\frac{P_{H_2O}}{P_{H_2}}\frac{1}{\gamma_{FeO}}e^{\Delta G^0/RT}}, \tag{1.6}$$

Eq. (1.6) correlates reduction ratio with slag ratio, gas composition, reaction temperature and activity coefficient of FeO. Therefore, the activity coefficient of FeO will definitely affect the material balance and hence energy balance of the suspension ironmaking process.

1.5. Scope of This Research Work

This work is about process simulation and economic analysis of the suspension ironmaking technology taking into consideration the effect of activity coefficient of FeO in slag. Mathematical models of activity coefficient of FeO in slag in the literature were first selected, reviewed, and assessed. The model that is the most appropriate to the suspension ironmaking process was chosen. Combining this selected model, Metsim simulation to calculate material and energy balance was conducted for the suspension ironmaking process under different conditions. At last, with the calculated results of material and energy balance, economic feasibility of the suspension ironmaking technology was analyzed.

Due to the consideration of effect of FeO activity coefficient in slag, compared to Pinegar's work, this study adopted the following changes:

(1). The reduction extent of iron oxide was reduced from 99% to 96%-98%;

(2). In simulating suspension ironmaking process with pure H_2, the recycled H_2 was considered to be saturated with water vapor at 30 ºC instead of being dry at 50 ºC. At the same time, the simulation flow sheet of suspension ironmaking process with pure H_2 was simplified by directly connecting recycling line to heat exchanger and removing two controllers;

(3). In simulating reformerless suspension ironmaking process with natural gas, the heat exchanger for preheating natural gas was relocated after the burner instead of after the main reactor, and 5% excess O_2 was mandated in the burner instead of in the offgas;

(4). In simulating suspension ironmaking process with SMR, 5% excess O_2 was mandated in the burner instead of in the offgas, and two controllers were added for automatic control of material flow amounts instead of manual adjustment.

CHAPTER 2

SELECTION OF A MATHEMATICAL MODEL FOR CALCULATING THE ACTIVITY COEFFICIENT OF FeO IN SLAG

2.1. Literature Research on Activity Coefficient of FeO in Slag

Henao and Itagaki [18] pointed out "thermodynamic information of activity and activity coefficient are important to the development of new metallurgical process. Furthermore, this information can assist in improving the computer simulation models." As indicated above, the activity coefficient of FeO in slag plays an important role in determining material balance and energy balance of the suspension ironmaking process. Therefore, obtaining reliable data of the activity coefficient of FeO in slag is of critical importance in the process simulation and economic analysis of the suspension ironmaking technology.

Activity coefficient can be obtained by experimental measurements and model calculation. Experimental measurements of FeO activity and activity coefficient in ironmaking and steelmaking slag can be tracked back as early as 1942, when Taylor and Chipman published experimental results of iso-activity lines in pseudo-ternary system ($CaO+MgO-SiO_2-FeO$) at 1600 °C under N_2 atmosphere in a rotating induction furnace. In 1970, Timucin et al.[19] measured FeO activity in $CaO-SiO_2-FeO-Fe_2O_3$ slag system

at 1450 °C and 1550 °C under atmosphere of CO-CO_2 ($p_{O2}=10^{-11}$ – 1 atm), and reported their results in a series of activity charts. Ogura et al.[20] measured FeO activity coefficient in CaO-SiO-FeO slag system at 1400 °C by electrochemical method in 1992. In 1988, Ohta et al.[21] developed a model for calculating FeO activity coefficient with theory and validated their model with experimental results measured in CaO-SiO_2-MgO-Al_2O_3-FeO slag system under Ar atmosphere at 1600 °C. Fujiwara et al.[22] conducted experimental measurement of activity coefficient of diluted FeO in CaO-Al_2O_3-SiO_2-FeO slag system at 1600 °C under CO-CO_2 atmosphere in 2000. Fredriksson et al.[23-24] determined FeO activity by experiment in binary slag systems of CaO-FeO, SiO_2-FeO and Al_2O_3-FeO at 1550-1600 °C and ternary slag systems of CaO-SiO-FeO, MgO-SiO_2-FeO, Al_2O_3-SiO_2-FeO at 1550 C-1650 °C under CO-CO_2-Ar atmosphere in 2004. Lu et al.[25] used the electrochemical method of solid electrolyte cells to measure FeO activity coefficient in a slag system CaO-SiO_2-Al_2O_3-MgO-FeO at 1400 °C in 2008.

Along with experimental measurement of FeO activity coefficient in slag, various theoretical and empirical models have also been developed to predict activity coefficient of FeO in slag. In 1993, based on a regular solution model, Ban-Ya [26] derived a mathematical expression of FeO activity coefficient in multicomponent slag by quadratic formalism. Park and Lee [27] calculated the activity coefficient of iron oxides using regular solution model and ionic model in 1996. Tao [28] developed a molecular interaction volume model to predict the activity of FeO in ternary molten slag system CaO-FeO-SiO_2 in 2006 and Meraikib [29] determine the activity coeffecient of total ferrous oxides in slag by using the theory of regular ionic solutions in 2008.

2.2. Mathematical Models of FeO Activity Coefficient Selected for Assessment

As discussed in the previous section, five models in the literature for predicting activity coefficient of FeO in slag were found: Meraikib's, Ban-Ya's, Ohta and Suito's, Tao's and Park and Lee's models.

Ohta and Suito's model [21] is an empirical model that was developed based on experimental data at 1600 °C. It cannot be used at other temperatures. Therefore, it is not appropriate to use this model for the current study of process simulation with various temperatures for the suspension ironmaking process. As such, this model will not be further assessed.

Tao's model [28] is applicable only to the CaO-SiO_2-FeO ternary slag system, which is far away from the proposed slag system of suspension ironmaking process. Besides, Tao's model is too complicated, many parameters of which need to be measured from binary slag systems. As a result, Tao's model will not be further evaluated either.

Meraikib's model [29] was developed to the calculate activity coefficient of total ferrous oxides in slag based on the theory of regular ionic solutions. The model correlates the activity coefficient of total ferrous oxides to slag temperature and composition. Expression of the model is given as

$$\ln \gamma_{FetO} = \frac{120.3}{T}\{10x_{CaO}(x_{Fe_tO} + 20.1x_{P_2O_5} - 1) + 25.1x_{Al_2O_3}(x_{Fe_tO} - 4.73x_{MnO} + 4.16x_{CaO} - 5.49x_{MgO} - 5.0x_{SiO_2} - 1) + 9.20x_{SiO_2}(4.54x_{MnO} - x_{Fe_tO} + 12.27x_{CaO} + 12.27x_{MgO} + 1)\} \quad (2.1)$$

In Eq. (2.1), γ_{FetO} is activity coefficient of total ferrous oxides, x_i is mole fraction of slag component *i*, and T is slag temperature. The total ferrous oxides is defined as

$$(Fe_tO) = (FeO) + 0.9\ (Fe_2O_3) \qquad (2.2)$$

Ban-Ya's model[26] was derived by quadratic formalism based on the regular solution model. The model is expressed by

$$\begin{aligned}\ln \gamma_{FeO} = \frac{1}{RT}\{&-18660x^2_{FeO1.5} + 7110x^2_{MnO} - 41840x^2_{SiO2} + 33470x^2_{MgO} - 31380x^2_{CaO} + 44930x_{FeO1.5}x_{MnO} \\ &- 93140x_{FeO1.5}x_{SiO2} + 17740x_{FeO1.5}x_{MgO} + 45770x_{FeO1.5}x_{CaO} + 40580x_{MnO}x_{SiO2} - 21340x_{MnO}x_{MgO} \\ &+ 67780x_{MnO}x_{CaO} + 58570x_{SiO2}x_{MgO} + 60670x_{SiO2}x_{CaO} + 102510x_{MgO}x_{CaO}\}(Joul)\end{aligned} \qquad (2.3)$$

In Eq. (2.3), γ_{FeO} is FeO activity coefficient, and other symbols have the same meaning as in Eq. (2.2).

Al_2O_3 is not present in Ban-Ya's model. When using Ban-Ya's model to calculate activity coefficient of FeO in CaO-SiO_2-Al_2O_3-MgO-FeO slag system, Al_2O_3 was combined with SiO_2.

Park and Lee's model is a regular solution model [27]. It is expressed by Eq. (2.4). All symbols in Eq (2.4) have the same meaning as in Eq. (2.3).

2.3. Criterion for Selecting the Most Appropriate Model

A measure is defined in this research to assist in assessing which model of the three listed in the previous section is the most accurate to predict the activity coefficient of FeO

$$\ln \gamma_{FeO} = \frac{1}{RT}\{-18670x^2_{FeO1.5} + 7120x^2_{MnO} - 41860x^2_{SiO2} + 33490x^2_{MgO} - 31400x^2_{CaO} - 31400x^2_{PO2.5} - 41020x^2_{AlO1.5} + 44960x_{FeO1.5}x_{MnO} - 93180x_{FeO1.5}x_{SiO2} - 21350x_{MnO}x_{MgO} + 45790x_{FeO1.5}x_{CaO} + 40600x_{MnO}x_{SiO2} + 67810x_{MnO}x_{CaO} + 82460x_{CaO}x_{AlO1.5} + 60700x_{SiO2}x_{CaO} + 102560x_{MgO}x_{CaO} + 39770x_{MgO}x_{PO2.5} + 58600x_{MgO}x_{SiO2} + 188370x_{CaO}x_{PO2.5} + 17750x_{MgO}x_{FeO1.5} + 63630x_{MgO}x_{AlO1.5} + 49810x_{AlO1.5}x_{MnO} + 44790x_{AlO1.5}x_{SiO2} + 189210x_{AlO1.5}x_{PO2.5} + 101470x_{AlO1.5}x_{FeO1.5} + 60700x_{MnO}x_{PO2.5} - 156980x_{SiO2}x_{PO2.5} - 64720x_{PO2.5}x_{FeO1.5}\}(Joule) \quad (2.4)$$

in slag under the conditions of the suspension ironmaking process. This measure is called a Square Root of Mean Sum of Squares of Differences (SRMSSD) between predicted and measured values of activity coefficients of FeO in slag.

Assume that there are *n* different slag samples. For each of these slag samples, the measured activity coefficient of FeO can be found from the literature. The activity coefficient of FeO can also be predicted from the slag composition and temperature using the three mathematical models listed above. SRMSSD then can be calculated by

$$SRMSSD = \sqrt{\sum_{i=1}^{n}(\gamma_{FeO,pi} - \gamma_{FeO,mi})^2 / n} \quad (2.5)$$

Here, n is the number of the γ_{FeO}, $\gamma_{FeO,pi}$ and $\gamma_{FeO,mi}$ are predicted and measured values of activity coefficient of FeO in slag for the *ith* sample, respectively.

This measure indicates that the smaller the SRMSSD value, the more accurately the model predicts the activity coefficient of FeO. Therefore, a model with the smallest SRMSSD value will be selected as the model to be used in this process simulation for the

suspension ironmaking process.

2.4. Selection of Experimental Data of Activity Coefficient of FeO Published in Literature

The suspension ironmaking process is expected to be operated under the conditions of temperature range between 1500 °C and 1600 °C, slag system with CaO, SiO_2, MgO, Al_2O_3, FeO and other minor components, and slag basicity CaO/SiO_2 around 1.2.

There are hundreds of experimental data of the activity coefficient of FeO in slag that can be found in literature. However, many of these data were obtained under conditions far away from the suspension iromaking process, and they should not be used for the model selection. In order to choose a model that is the most appropriate to the suspension ironmaking process, only experimental data measured under the conditions close to those expected for the suspension ironmaking process have been selected.

Sixteen experimental data point of activity coefficient of FeO in slag have been selected and used to evaluate the mathematical models of activity coefficient of FeO. The data are collected in Table 2.1.

2.5. Experimental Measurement of Activity Coefficient of FeO In $CaO\text{-}SiO_2\text{-}MgO\text{-}Al_2O_3\text{-}FeO$ Slag System in This Study

From equation (1.4), the activity coefficient of FeO can be derived as follows:

$$\gamma_{FeO} = \frac{p_{H_2O}}{p_{H_2}} \frac{1}{k x_{FeO}} \qquad (2.6)$$

Great efforts were made in this research to directly measure the activity coefficient

Table 2.1. Selected experimental data of activity coefficient of FeO in literature

Researcher	**Temperature** °C	**FeO** %	**SiO_2** %	**CaO** %	**MgO** %	**Al_2O_3** %	**CaO% /SiO_2%**	γ_{FeO}
Taylor and Chipman [30]	1600	12.42	46.15	34.46	6.97		0.75	2.30
		12.46	41.67	38.89	6.99		0.93	2.70
		12.49	37.95	42.55	7.01		1.12	3.20
		12.51	34.88	45.58	7.02		1.31	3.60
Fridriksson and Seetharaman [24]	1600	8.52	46.83	44.65			0.95	1.43
		7.32	46.95	45.73			0.97	1.33
		7.32	46.95	45.73			0.97	1.04
		8.52	46.83	44.65			0.95	1.02
		3.67	54.27	42.05			0.77	1.00
		3.68	53.29	43.04			0.81	1.00
Tao[28]	1600	29.19	36.62	34.18			0.93	2.00
		22.26	40.21	37.53			0.93	2.13
		16.65	43.07	40.29			0.94	2.16
		10.19	46.46	43.36			0.93	2.38
		4.42	49.44	46.14			0.93	2.78
		29.34	29.44	41.22			1.40	2.40

of FeO in CaO-SiO_2-MgO-Al_2O_3-FeO slag system by experiments with a high-temperature vertical furnace. A 99.8% pure MgO crucible was used to hold 30g electrolytic iron and 8g pre-made slag. H_2 and H_2O vapor mixture were injected into the furnace to keep p_{H2O}/p_{H2}=0.5. The experimental temperature was 1550 °C. Equilibrium slag composition was analyzed and activity coefficient of FeO was calculated using Eq. (2.6). The experimental result is summarized in Table 2.2.

2.6. Selection of the Most Appropriate Model of FeO Activity Coefficient for This Simulation

Using data of slag composition and experimental temperature listed in Tables 2.1 and 2.2, the activity coefficient of FeO has been predicted from models (2.1), (2.3) and (2.4). The results are listed in Table 2.3.

Table 2.2. Measured activity coefficient of FeO in this study

Temperature, °C	**FeO %**	**SiO_2 %**	**CaO %**	**MgO %**	**Al_2O_3 %**	**CaO%/SiO_2%**	**γ_{FeO}**
1550	16.34	28.67	29.01	18.61	7.37	1.01	3.09

Table 2.3. Measured and predicted values of activity coefficient of FeO

Measured	**Predicted**			**Measured**	**Predicted**		
	Meraikib's	**Ban-Ya's**	**Park & Lee's**		**Meraikib's**	**Ban-Ya's**	**Park & Lee's**
2.3[a]	4.46	1.29	1.29	1[b]	5.53	0.8	0.8
2.7[a]	4.17	1.36	1.36	2[c]	2.73	0.89	0.81
3.2[a]	3.86	1.38	1.38	2.13[c]	3.25	0.88	0.81
3.6[a]	3.57	1.38	1.38	2.16[c]	3.75	0.86	0.86
1.43[b]	4.65	0.84	0.84	2.38[c]	4.48	0.84	0.86
1.33[b]	4.77	0.84	0.84	2.78[c]	5.26	0.83	0.86
1.04[b]	4.77	0.84	0.84	2.4[c]	2.45	0.88	0.86
1.02[b]	4.64	0.84	0.84	**3.09[d]**	2.54	2.49	2.92
1[b]	5.56	0.79	0.79				

a. Data from Taylor and Chipman[30]
b. Data from Fredriksson and Seetharaman[24]
c. Data from Tao[28]
d. Data from this study

Using the measured and predicted values of the activity coefficient of FeO in Table 2.3, the SRMSSD value for each model has then been calculated and tabulated in Table 2.4.

The calculated results show that Park and Lee's model has the smallest SRMSSD value. Besides, from Table 2.3, one can see that Park and Lee's model gave the best prediction to the FeO activity coefficient in the slag sample tested in this study (predicted value 2.92 versus measured value 3.09). Consequently, Park and Lee's model has been selected to calculate activity coefficient of FeO in slag in this research.

2.7. Activity Coefficient of FeO in Slag Used in This Process Simulation

As discussed above, Park and Lee's model was selected to calculate the activity coefficient of FeO in slag in the process simulation of suspension ironmaking process. The calculation was performed with the experimental slag composition listed in Table 2.2, and the calculated results are summarized in Table 2.5.

Table 2.4. SRMSSD values for the models being evaluated

Model	**Meraikib's**	**Ban-Ya's**	**Park & Lee's**
SRMSSD	2.58	1.22	1.21

Table 2.5. FeO activity coefficient used in Metsim process simulation

Temperature ^{o}C	**γ_{FeO}**	**H_2 Driving Force**	**β**
1500	3.01		
1550	2.92		
1600	2.84	0.5-2.0	0.967-0.990

CHAPTER 3

FLOW DIAGRAMS OF THE SUSPENSION IRONMAKING PROCESS WITH DIFFERENT H_2 SOURCES

3.1. Simulation Scope

In the suspension ironmaking process, reduction of magnetite iron ore concentrate into iron undergoes two steps. The first step is to reduce magnetite into wustite, and the second step is from wustite to iron. These reducing reactions with hydrogen are expressed in Eqs. (3.1) and (3.2).

$$Fe_3O_4 + H_2 = 3FeO + H_2O_{(g)} \quad (3.1)$$

$$FeO + H_2 = Fe + H_2O_{(g)} \quad (3.2)$$

Accordingly, there are two types of suspension ironmaking processes: one-step and two-step. In the one-step suspension ironmaking process, magnetite concentrate is fed into a suspension ironmaking reactor and reactions (3.1) and (3.2) take place and finish in a single reactor. On the other hand, in the two-step suspension ironmaking process, reactions (3.1) and (3.2) occur in two different suspension ironmaking reactors. Magnetite concentrate and offgas from the first reactor are fed into the second reactor,

where magnetite is reduced into wustite at 900 °C. The wustite is then hot charged into the first reactor, where wustite is reduced into iron at 1500 - 1600 °C.

A commercial scale suspension ironmaking plant producing one million ton hot iron per year has been simulated**.** Six processes, based on different hydrogen sources, have been considered. They are one-step pure H_2 process, two-step pure H_2 process, one-step reformerless natural gas process, two-step reformerless natural gas process, one-step steam-methane-reforming-producing H_2 process (SMR-H_2) and one-step steam methane-reforming-producing syngas process (SMR-syngas).

3.2. Flow Diagrams of Suspension Ironmaking Process with Pure H_2

In this simulation, production of H_2 is not integrated with the suspension ironmaking process. In other words, the origin of H_2 is not considered.

Figures 3.1 and 3.2 show flow diagrams of simulated suspension ironmaking processes with pure H_2. Figure 3.1 is for the one-step process and Figure 3.2 is for the two-step process. As indicated in Figure 3.1, iron ore concentrate, flux, preheated hydrogen and oxygen are fed into a single suspension ironmaking reactor. Part of the input hydrogen is burnt with oxygen. Along with the sensible heat, which is brought into the reactor by the preheated hydrogen, the heat generated from the combustion reaction will provide energy for the ironmaking process. Iron oxides are reduced into liquid iron and impurities in the iron ore concentrate react with flux and form liquid slag. The offgas emitted from the reactor is at high temperature and contains considerable sensible heat. It first goes through a heat exchanger to preheat fresh and recycled hydrogen, and then passes through a waste heat boiler to have its waste heat further

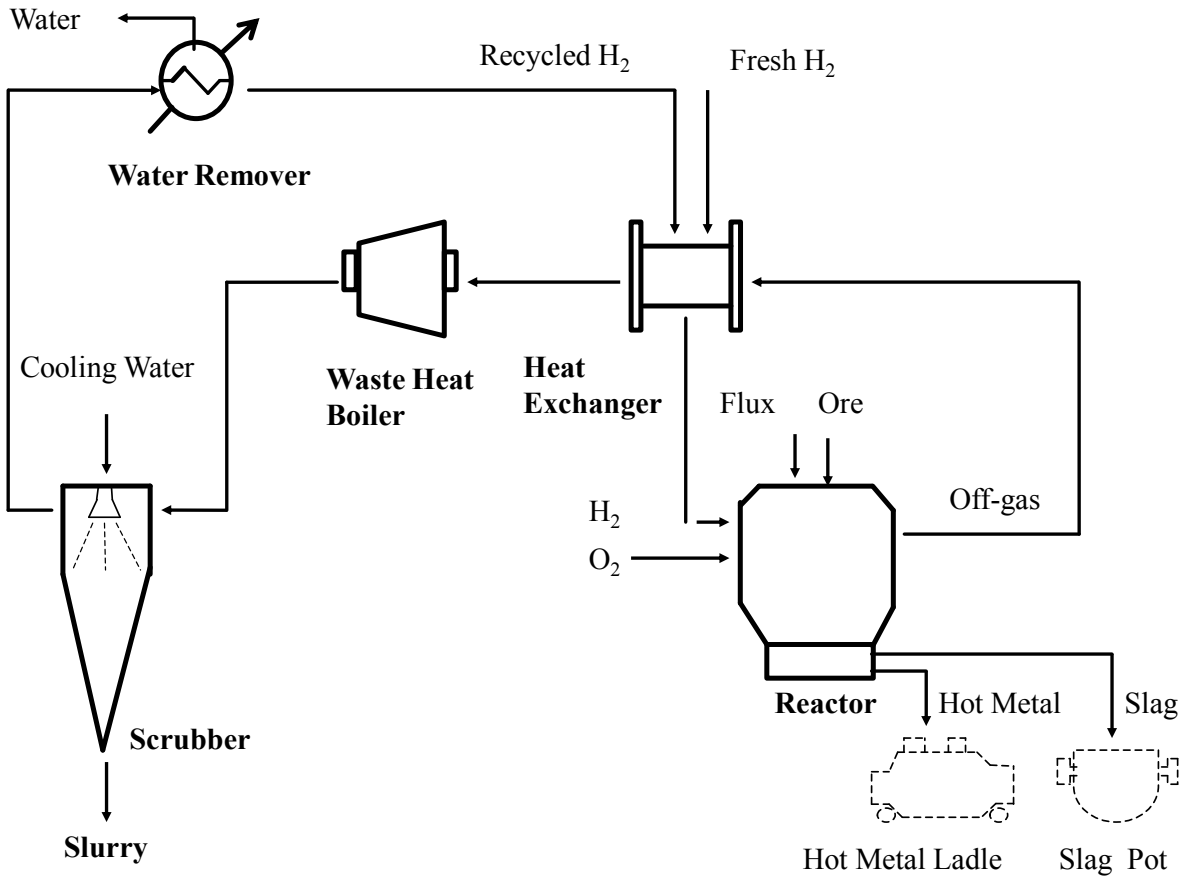

Figure 3.1. Flow diagram of one-step suspension ironmaking process with pure H_2

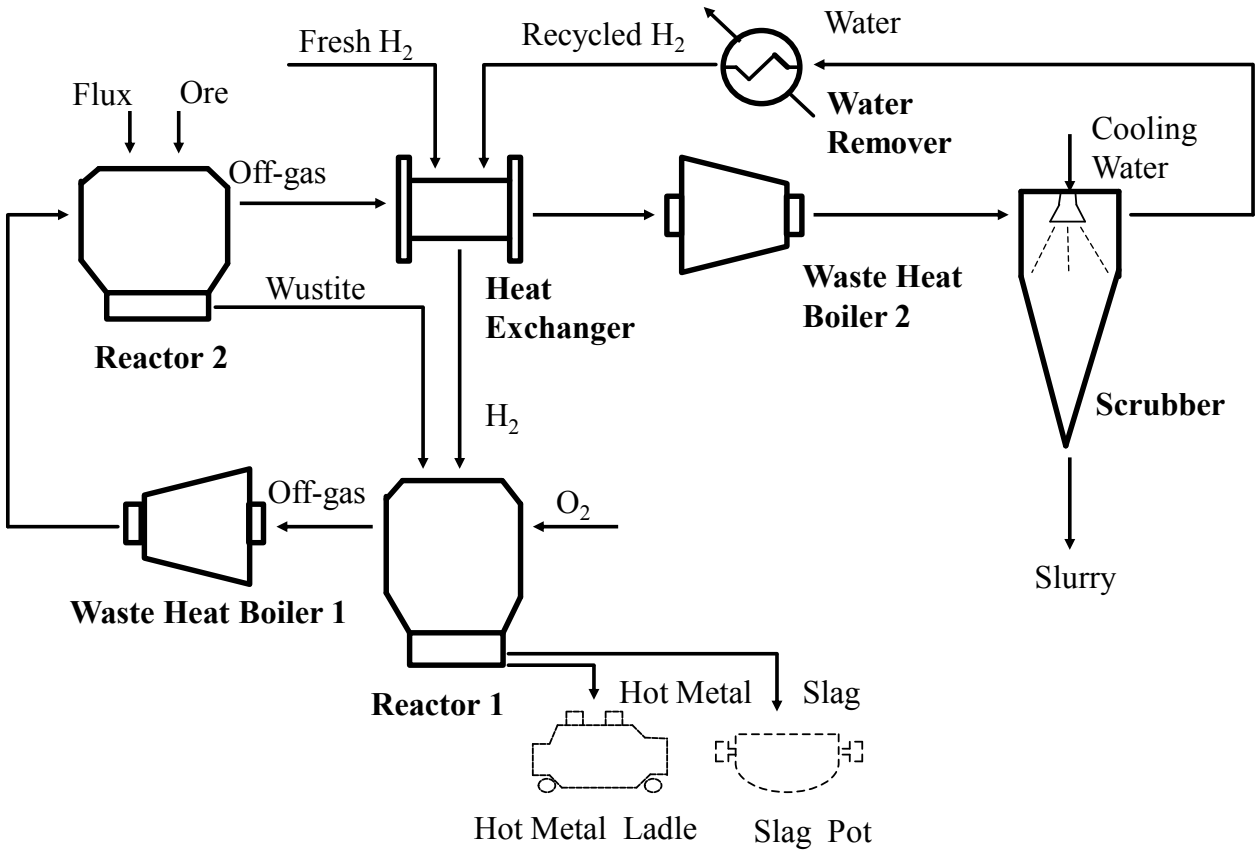

Figure 3.2. Flow diagram of two-step suspension ironmaking process with pure H_2

recovered. After most of the waste heat is recovered, the offgas is cleaned by a scrubber. The clean offgas is finally dewatered, mixed with fresh hydrogen and preheated in the heat exchanger. It is clear that in the one-step suspension ironmaking process with pure H_2, there are no gas emissions, except slurry from the wet scrubber and water from water remover.

Different from the one-step suspension ironmaking process, as illustrated in Figure 3.2, in the two-step suspension ironmaking process with pure H_2, wustite, flux, preheated hydrogen and oxygen are fed into reactor one. Part of the preheated hydrogen is burnt with oxygen to provide enough heat for reactions and phase transformations in reactor one. Wustite is reduced by hydrogen into liquid iron and liquid slag is formed in reactor one. Offgas emitted from the reactor goes through a waste heat boiler and decreases its temperature to about 900 °C. The offgas is then input into reactor two with iron ore concentrate and flux. Iron ore concentrate is reduced into wustite by hydrogen and flux is preheated in the reactor. Offgas emitted from reactor two is treated in the same way as in the one-step suspension ironmaking process with pure H_2.

3.3. Flow Diagrams of Reformerless Suspension Ironmaking Process with Natural Gas

In this simulation, natural gas is considered as a H_2 source and is directly used in the suspension ironmaking process.

Figures 3.3 and 3.4 show flow diagrams of simulated suspension ironmaking process with natural gas as a hydrogen source. Figure 3.3 is for the one-step process and Figure 3.4 is for the two-step process. As seen in Figure 3.3, iron ore concentrate,

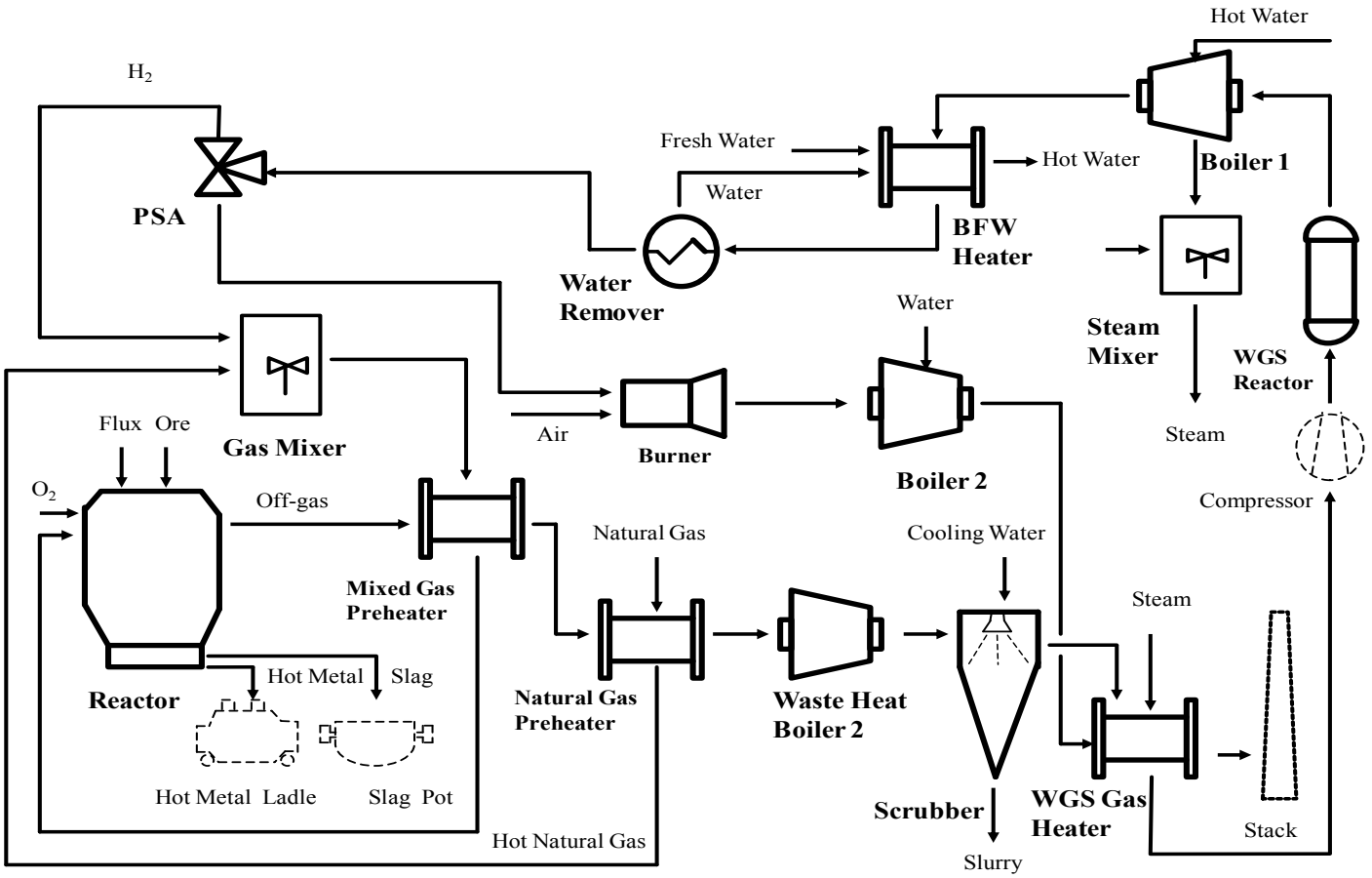

Figure 3.3. Flow diagram of one-step reformerless suspension ironmaking process with natural gas

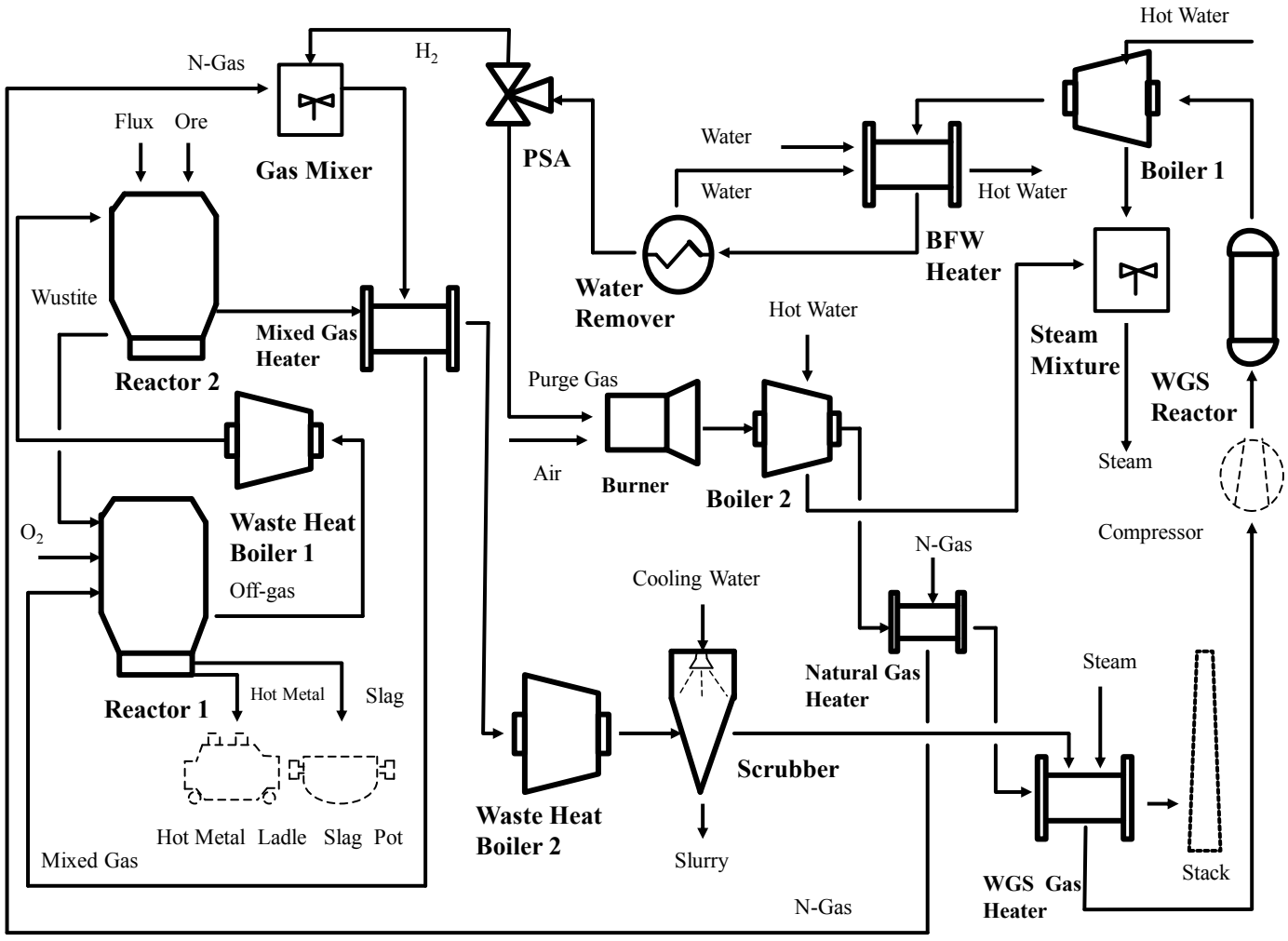

Figure 3.4. Flow diagram of two-step reformerless suspension ironmaking process with natural gas

flux, preheated gas mixture of fresh natural gas and hydrogen, as well as oxygen are fed into a single suspension ironmaking reactor. Part of the natural gas is combusted with oxygen. Along with the sensible heat, which is brought into the reactor by the preheated gas mixture, the heat generated from the combustion reaction will provide energy for the ironmaking process. Iron oxides are reduced into liquid iron and impurities in the iron ore concentrate react with flux and form liquid slag. The offgas emitted from the reactor is at high temperature and contains considerable sensible heat. It first goes through a heat exchanger to preheat the gas mixture of warmed fresh natural gas and hydrogen, and then passes through the second heat exchanger to warm fresh natural gas. Waste heat in the offgas is further recovered in a waste heat boiler. After that, the offgas is cleaned by a wet scrubber. The clean offgas is then mixed with steam and preheated. The mixture of offgas and steam is then compressed and pumped into a water gas shift (WGS) reactor where water reacts with CO and hydrogen is produced. The WGS gas passes through a waste heat boiler and a heat exchanger for waste heat recovery. After water is removed from the WGS gas, hydrogen in the gas is separated. The separated hydrogen is mixed with warmed natural gas, preheated and fed into the suspension ironmaking reactor. The remaining WGS gas is burnt to produce hot offgas. This hot offgas is then used to produce steam in a waste heat boiler and to supply heat for the WGS gas heater. After its heat is recovered, the burnt WGS gas is released into the air. Besides slurry and condensed water, offgas is also an emission from the reformerless suspension ironmaking process with natural gas.

As shown in Figure 3.4, in the two-step reformerless suspension ironmaking process with natural gas, wustite and flux discharged from reactor two, preheated gas

mixture of warmed natural gas and hydrogen, and oxygen are fed into reactor one. Part of the preheated natural gas is burnt with oxygen to provide enough heat for reactions and phase transformations in reactor one. Wustite is reduced into liquid iron by hydrogen and natural gas. At the same time, liquid slag is formed in reactor one. Offgas emitted from the reactor goes through a waste heat boiler first and then fed into reactor two. Iron ore concentrate and flux are charged into reactor two and iron oxides are reduced to wustite by gas from reactor one. The offgas emitted from reactor one is treated in the same way as in the one-step reformerless suspension ironmaking process with natural gas as described above.

3.4. Flow Diagrams of Suspension Ironmaking Process with SMR-H_2 or SMR-Syngas

Steam-methane reforming (SMR) is the best available technology for producing H_2 from natural gas. Though up-to-date SMR technology has not been sufficiently cheap, to be complete, the suspension ironmaking process integrated with SMR-H_2 was simulated in the current research. Besides, the suspension ironmaking process integrated with SMR-syngas was also simulated. However, only the one-step suspension ironmaking process with SMR-H_2 or SMR-syngas was considered.

Figure 3.5 illustrates a flow diagram of the simulated one-step suspension ironmaking process with SMR-H_2. Iron ore concentrate, flux, preheated H_2 and oxygen are fed into a single suspension ironmaking reactor. Part of the input H_2 is burnt with oxygen. Along with the sensible heat, which is brought into the reactor by the preheated H_2, the combustion heat will provide energy for the ironmaking process. Iron oxides are reduced into liquid iron and impurities in the iron ore concentrate react with flux and

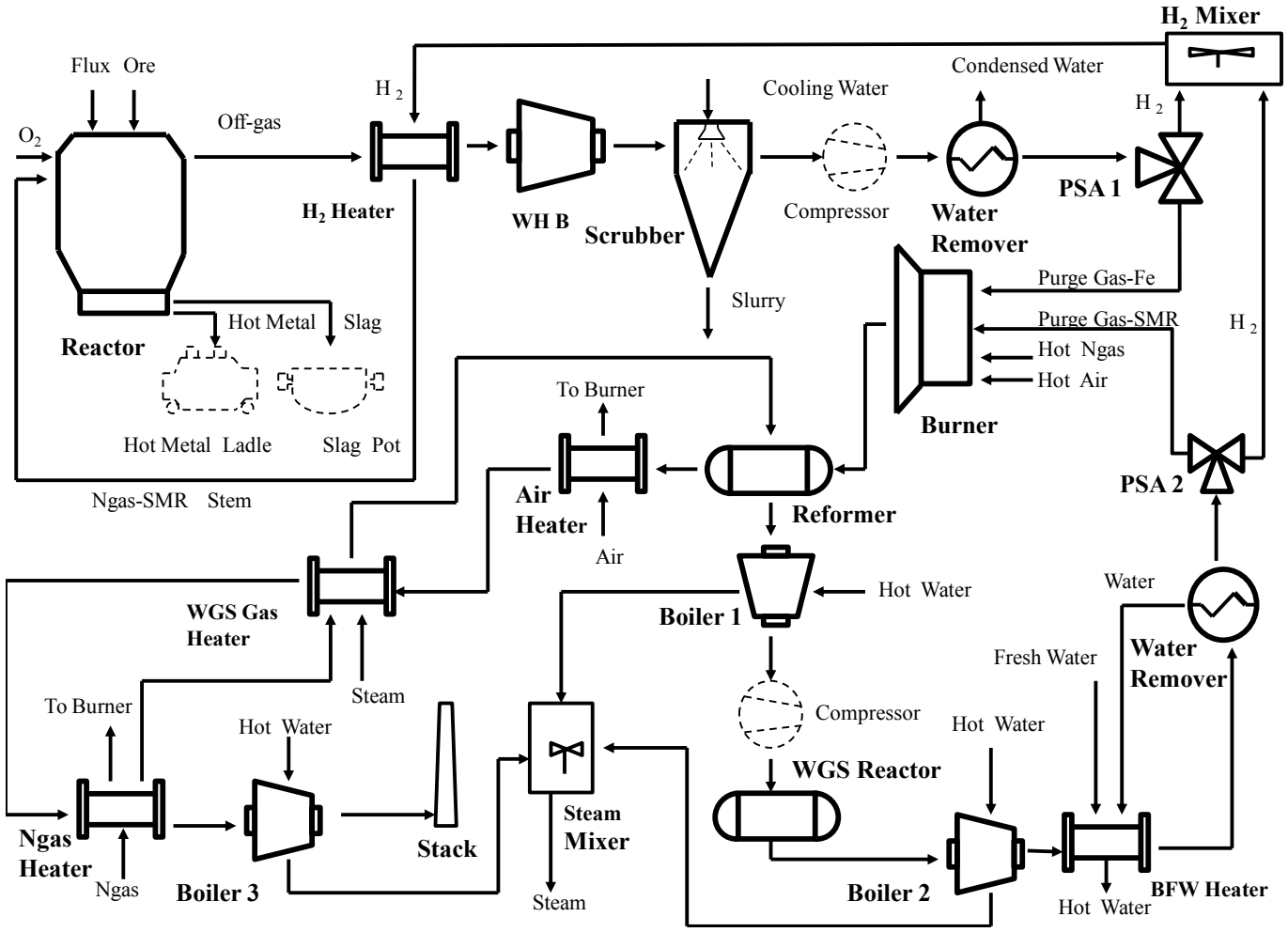

Figure 3.5. Flow diagram of one-step suspension ironmaking process with SMR-H_2

form liquid slag. The offgas emitted from the reactor first goes through a hydrogen heater to preheat mixed hydrogen generated and recycled in this integrated process. Afterwards, waste heat in the offgas is further recovered by a waste heat boiler. The offgas is then cleaned by a wet scrubber. The clean offgas is compressed, passes through a water remover, and is fed into a pressure swing adsorption (PSA) unit to separate H_2 from the offgas. The separated H_2 from the offgas is mixed with H_2 from SMR, preheated and fed into the suspension ironmaking reactor.

Natural gas is preheated by the first heater and then with steam by the second heater. The preheated mixture of natural gas and steam is fed into a reformer. Reformed natural gas is discharged from the reformer and compressed into water gas shift (WGS) reactor. Product of the WGS reactor passes through a boiler, a heater and a water remover, and fed into PSA 2 to separate H_2. The separated H_2 is mixed with the H_2 from PSA 1, preheated and fed into the suspension ironmaking reactor. The remaining gas from both PSA 1 and PSA 2 is burnt in a burner with hot natural gas (380 °C) and hot air (800 °C). The hot waste gas is to heat the reformer, and three heaters for air, mixture of natural gas and steam and raw natural gas.

Figure 3.6 shows a flow diagram of the suspension ironmaking process integrated with SMR-sysgas, which is similar to Figure 3.5 except that (1) syngas, not pure H_2, is fed into the suspension ironmaking reactor; (2) there is no water gas shift reaction after the natural gas is reformed; and (3) there is no PSA separation of reformed natural gas for H_2

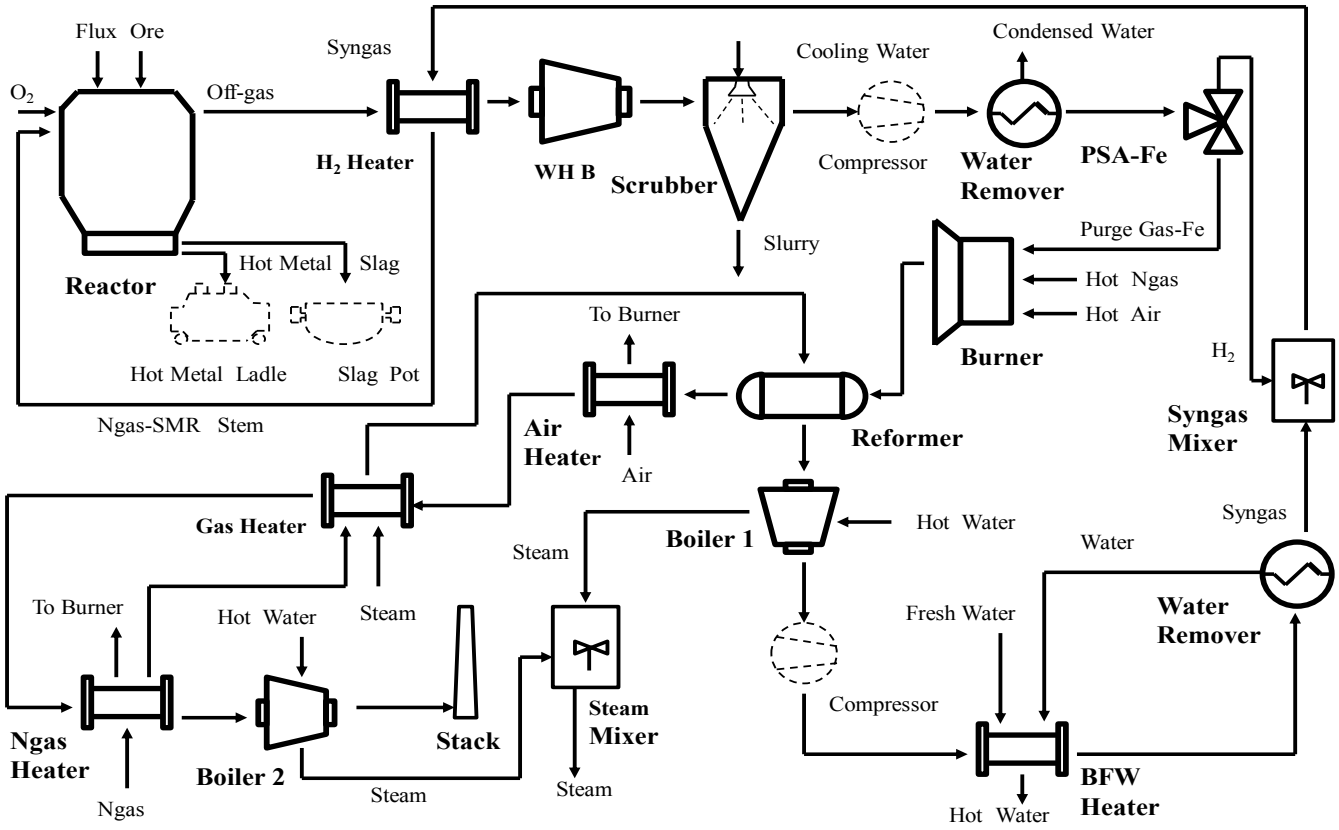

Figure 3.6. Flow diagram of one-step suspension ironmaking process with SMR-syngas

CHAPTER 4

SIMULATION OF THE SUSPENSION IRONMAKING PROCESS

4.1. Metsim Simulation Software

Metsim is a simulation software package for simulating mineral processing, coal preparation, metallurgical process and chemical reaction process. It can be used for steady state or dynamic simulation, batch or continuous simulation, equipment sizing, and model-based control and so on [31].

Metsim simulation can be visualized by block diagrams that are composed of standard operation units, streams and controllers. Operation units are used to simulate reactors, scrubbers, boilers, heat exchangers, etc. Chemical reactions and phase changes can be specified in the operation units to certain extend. Streams represent material flows with mass and energy, and the materials can be in single phases or multiphases. Controllers can be inserted at selected transfer points to change unit inputs to maintain specified outputs, such as temperature, composition, material flow rate, and so forth.

Operation units can be connected together by streams to form a process flow sheet. Mass, energy, and composition of output are automatically calculated out and can be exported to Excel files for further analysis.

In this study, Metsim is used to construct different configurations of the suspension ironmaking process under steady, continuous conditions and to calculate material balance

and energy balance.

4.2 Metsim Simulation Block Diagrams for the Suspension Ironmaking Process with Different H_2 Sources

As indicated above, Metsim simulation can be visualized by Metsim simulation block diagrams which contain units, streams and controllers. The six flow diagrams discussed in Chapter 3 have been converted into Metsim simulation block diagrams, which are grouped in Appendix A. Units and streams corresponding to these Metsim block diagrams are explained in the tables of Appendices B and C, respectively. Reactions taking place in these simulated processes are listed in the tables of Appendix D, where reaction extent of FeO reduction by H_2 is determined by Eq. (1.6) and other reaction extents calculated through thermodynamics with HSC software.

4.3.Base Conditions of Simulation

Base conditions in this simulation include production of iron, operating temperature, reducing gas preheating temperature and hydrogen excess driving force which is defined as the following[17]:

$$\mathrm{H_2\ Excess\ Driving\ Force} = \frac{(\frac{n_{H_{2,off}}}{n_{H_2O_{,off}}}) - (\frac{n_{H_{2,eq}}}{n_{H_2O_{,eq}}})}{(\frac{n_{H_{2,eq}}}{n_{H_2O_{eq}}})} \qquad (4.1)$$

$n_{H2,off}$ and $n_{H2O,off}$ are the moles of hydrogen and water vapor in the offgas, and $n_{H2,eq}$ and $n_{H2O,eq}$ are the moles of hydrogen and water vapor at the equilibrium of reaction

$FeO + H_2 = Fe + H_2O(g)$. The base conditions for simulating the suspension ironmaking process are summarized in Table 4.1.

4.4.Process Heat Loss

Heat loss in pipes (represented by steams) was not considered in this study. Heat loss in heat exchangers and water gas shift reactor was assumed 5% of sum of heat input and heat generated in the reactor.

Heat loss from ironmaking reactors and prereduction reactors was taken from Pinegar et al.[13-14] and the data are listed in Table 4.2.

Table 4.1. Base simulation conditions

Process	**Production** (million ton/year)	**Operating Temperature** (˚C)	**Preheating Temperature of Reducing Gas** (˚C)*	**H_2 Excess Driving Force****
1-step	1	1500	900	0.5
2-step	1	1500	750	0.5

*H_2 is the reducing gas in pure H_2 process, reformerless natural gas process and SMR- H_2 process, while syngas is the reducing gas in SMR-syngas process.
**H_2 excess driving force is still used for SMR-syngas process.

Table 4.2. Heat loss rates for the commercial-scale ironmaking reactor and the pre-reduction reactor

Operating Temperature in the Ironmaking Reactor	**Reactor Heat Loss Rate** (GJ/h)		
	1-step Process	**2-step Process**	
	Ironmaking Reactor	**Ironmaking Reactor**	**Prereduction Reactor**
1500^{o}C	108	82.6	25.5
1550^{o}C	112	85.4	25.5
1600^{o}C	116	88.2	25.5

CHAPTER 5

SIMULATED RESULTS AND DISCUSSION

5.1. Results for the Suspension Ironmaking Process with Pure H_2

Simulated material balance for a one-million ton hot iron per year, suspension ironmaking plant with pure H_2 is listed in Table 5.1. Material balance for an average conventional blast furnace ironmaking process is also listed in the same table for comparison.

From Table 5.1, one can see that (1) the suspension ironmaking process with pure H_2 would consume less than half the raw materials than conventional blast furnace ironmaking process; (2) the suspension ironmaking process with pure H_2 would have no offgas emissions, and in opposite, in blast furnace ironmaing process, offgas takes more than 75% of total output; (3) slag in the suspension ironmaking process with pure H_2 would be less than in the blast furnace ironmaking process; (4) the two-step suspension ironmaking process with pure H_2 will consume less hydrogen and oxygen than the one-step suspension ironmaking process.

In the suspension ironmaking process with pure H_2, hydrogen is the only source for heating and reducing while in the cited blast furnace ironmaking process, carbon is the main source for heating and reducing. There are four principal reasons for the much smaller material flow rate in the suspension ironmaking process with pure H_2 than in

Table 5.1. Material balance for a one–million ton hot iron per year suspension ironmaking plant with pure H_2, ton/tHI

Items		1-step Process	2-step Process	BF [a] Process
INPUT	Hydrogen	0.11	0.09	
	Oxygen	0.46	0.32	0.68
	Iron ore	1.5 (magnetite)	1.5 (magnetite)	1.43 (hematite)
	Flux	0.06	0.06	0.29
	Coke			0.46
	Total-Ironmaking	**2.13**	**1.97**	**5.07**
	Cooling water for scrubber[b]	19.97	17.06	
OUTPUT	Hot iron	1	1	1.05 (contains 4.5% C)
	Slag	0.17	0.17	0.21
	Condensed water vapor	0.96	0.8	
	Total discharged gas			3.81
	CO_2			1.6[c]
	N_2			2.21
	Total Ironmaking[d]	**2.13**	**1.97**	**5.07**
	Cooling water in slurry	20.77	17.75	
	CO_2 from $CaCO_3$ and $MgCO_3$ calcination	0.04	0.04	

a. All BF ironmaking process data are from Pinegar, et al. [13-14].
b. The cooling water is used for off-gas cleaning and water vapor condensation in suspension process.
c. This data do not include the carbon dioxide emission from ore/coke preparation.
d. If the temperature of molten iron and slag is 1600 ˚C, the total material consumption will be 2.22 and 2.04 t/tHI for one-step and two-step, respectively

blast furnace ironmaking process: (1) pure O_2 is injected into furnace instead of air; (2) H_2 is much lighter than carbon; (3) coke contains 5% or more ash and considerable sulfur; (4) ash and sulfur in coke require extra flux, which also causes higher slag volume in blast furnace ironmaking process.

Water vapor is a product of heating and reducing in the suspension ironmaking process and it would condense after cooled, whereas CO and CO_2 are products in the blast furnace ironmaking process and they are emitted into the atmosphere after they are burned. Therefore, the suspension ironmaking process with pure H_2 will not have any offgas emissions, but the blast furnace ironmaking process is always having an offgas emission issue and high CO_2 footprint.

A little less consumption of H_2 in the two-step suspension ironmaking process than in the one-step suspension ironmaking process suggests improvement of utilization efficiency of H_2 in the two-step suspension ironmaking process.

Corresponding to Table 5.1, Table 5.2 lists energy balance for the simulated suspension ironmking process with pure H_2 and the cited blast furnace ironmaking process. It can be seen that (1) in comparison to the blast furnace ironmaking process, the suspension ironmaking process with pure H_2 requires much less energy supply; (2) the major energy saving for the suspension ironmaking process with pure H_2 is due to the reason that unlike blast furnace ironmaking process, the suspension ironmaking process can directly use iron ore concentrate and does not need to consume energy for producing pellets/sinter and coke from iron ore and coal; (3) the two-step suspension ironmaking process is more energy-efficient than the one-step suspension ironmaking process, and this explains why the two-step suspension ironmaking process consumes less hydrogen

Table 5.2. Energy balance for a one-million ton hot iron per year suspension ironmaking plant with pure H_2, GJ/tHI

Item		**1-step Process**	**2-step Process**	**BF Process[a]**
INPUT	Fuel combustion	9.33[b]	6.76[b]	8.33
	Heat recovery	-3.06	-1.19	-1.32[f]
	Subtotal	6.27	5.57	7.01
	Energy input for ore/coke preparation			5.68
	Total Ironmaking[g]	**6.27**	**5.57**	**12.7**
OUTPUT	Reduction	0.91	0.91	2.09
	Heat of reduction and slag formation	0.92	0.92	-0.16
	Sensible heat of hot iron	1.27 (1500°C)[d]	1.27 (1500°C)[d]	1.35 (1600°C)
	Sensible heat of slag	0.29 (1500°C)[d]	0.29 (1500°C)[d]	0.47 (1600°C)
	Slurry (H_2O(l))	2.17	1.85	
	Sensible heat of offgas			0.26 (90°C)
	Removed water vapor	0.003	0.002	
	$CaCO_3$ decomposition			0.33

Table 5.2 Continued

OUTPUT	Heat loss in the reactor	0.8	0.8	2.6
	Heat loss in the heat exchanger	0.38[d]	0.15[d]	0.07[f] (heat loss in heat recovery)
	Heat loss in water remover	0.44	0.29	
	Subtotal	**6.27**	**5.57**	**7.01**
	Pelletizing			3.014
	Sintering			0.654
	Cokemaking			2.024
	Total Ironmaking[g]	**6.27**	**5.57**	**12.7**
	$CaCO_3$ and $MgCO_3$ decomposition at 1000°C	0.26[c]	0.26[c]	

a. All BF ironmaking process data are from Pinegar et al.[13-14], in which energy balance was calculated by METSIM based on the material balance and at operating temperature of 1600˚C.
b. Fuel combustion energy was calculated by adding the energy of water vapor condensation to gas combustion. The higher heating value of H_2 gas was used for the calculation. If the lower heating value is used, the total energy requirements for the one-step and two-step processes will be 3.94 and 3.63 GJ/tHI respectively.
c. The energy needed for calcinating flux ($CaCO_3$ and $MgCO_3$) to generate CaO and MgO was calculated by METSIM at 1000 ˚C.
d. Heat losses in a heat exchanger were assumed to be 5% of the total sensible heat of input streams.
e. If the temperature of molten iron and slag is 1600 ˚C, the total energy requirements for the one-step and two-step processes will be, respectively, 6.76 and 5.94 GJ/ton using high heating value.

than the one-step suspension ironmaking process.

The effect of preheating temperature and H_2 excess driving force on hydrogen consumption is also simulated. The results are shown in Figures 5.1 and 5.2 and summarized as (1) the two-step suspension ironmaking process consumes less H_2 and energy than the one-step suspension ironmaking process; (2) a higher preheating temperature will result in less consumption of H_2; (3) a higher operating temperature of the ironmaking reactor will require higher consumption of H_2; (4) higher H_2 excess driving force will correspond to higher H_2 consumption rate and higher energy consumption. The effect of H_2 excess driving force on energy consumption is illustrated in Figure 5.3.

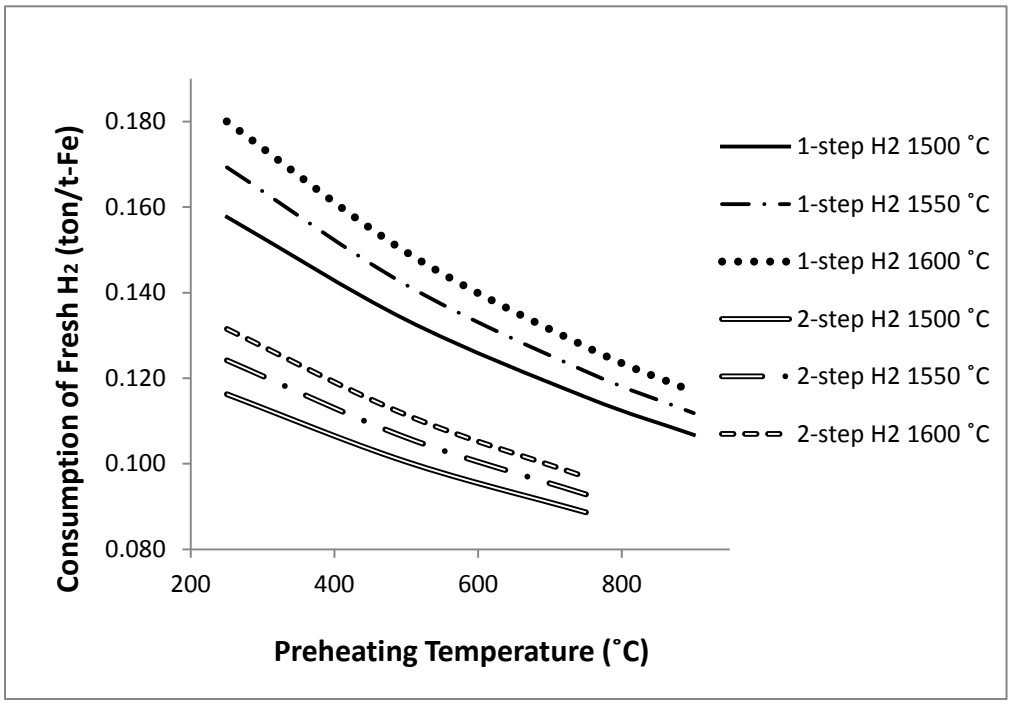

Figure 5.1. Effect of preheating temperature on H_2 consumption rate in pure H_2 suspension ironmaking process

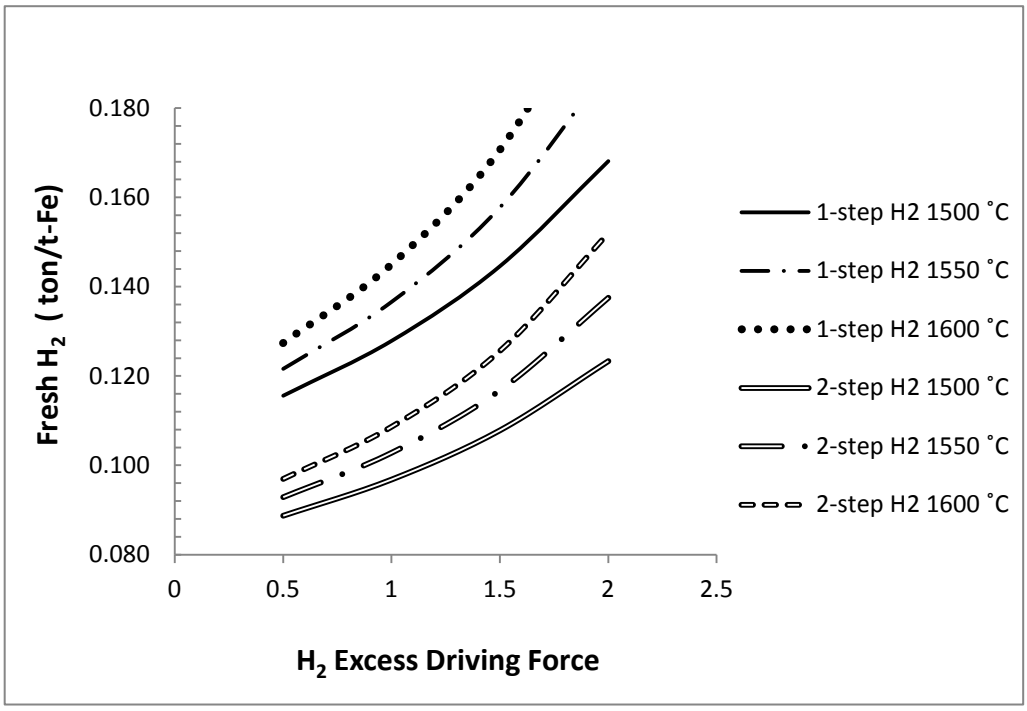

Figure 5.2. Effect of H_2 excess driving force on H_2 consumption rate in pure H_2 suspension ironmaking process

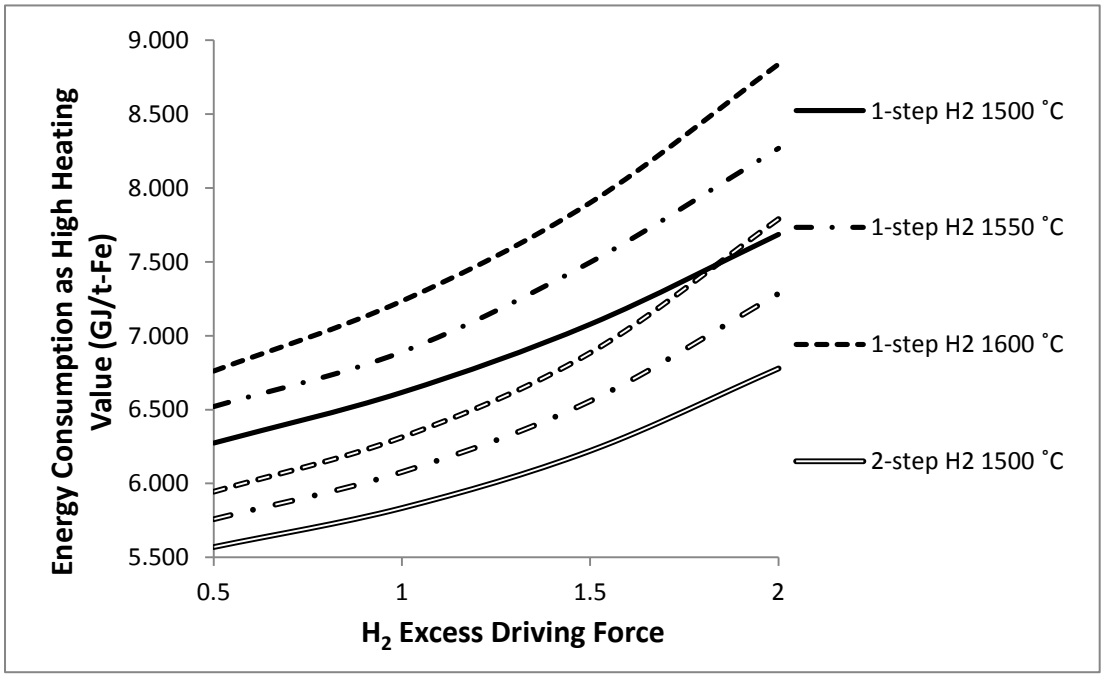

Figure 5.3. Effect of H_2 excess driving force on energy consumption in pure H_2 suspension ironmaking process

5.2. Results for the Reformerless Suspension Ironmaking Process with Natural Gas

Material balance and energy balance for the reformerless suspension ironmaking process with natural gas are tabulated in Tables 5.3 and 5.4. From these tables, it can be seen that (1) the reformerless suspension ironmaking process with natural gas emits around 36% less CO_2 than cited blast furnace ironmaking process; (2) the two-step suspension ironmaking process consumes around 22% less natural gas than the one-step suspension ironmaking process; (3) compared to cited blast furnace ironmaking process, the reformerless suspension ironmaking process with natural gas consumes 30-41% less energy; (4) the two-step suspension ironmaking process is more energy-efficient than the one-step suspension ironmaking process.

The effect of H_2 excess driving force on natural gas consumption and energy consumption is also simulated and plotted in Figures 5.4 and 5.5 It is clear that similar to the suspension ironmaking process with pure H_2, (1) higher H_2 excess driving force will result in higher natural gas and energy consumption; (2) the two-step suspension ironmaking process consumes less natural gas and requires less energy input than the one-step suspension ironmaking process; (3) higher operating temperature will need higher natural gas and energy consumption.

5.3. Results for the Suspension Ironmaking Process with SMR-H_2 and SMR-Syngas

Simulated results of material balance and energy balance for the suspension ironmaking process with one-step SMR-H_2 and SMR-syngas are listed in Tables 5.5 and 5.6. The results show that (1) the suspension ironmaking process with one-step SMR-H_2

Table 5.3. Material balance for the reformerless suspension ironmaking process with natural gas, ton/tHI

Item		1-step Process	2-step Process	BF Process[a]
INPUT	Natural gas	0.37	0.29	
	Oxygen	0.8	0.59	0.68
	Iron ore	1.5 (magnetite)	1.5 (magnetite)	1.43 (hematite)
	Flux	0.06	0.06	0.29
	Nitrogen			2.21
	Coke			0.46
	Fresh water	2.65	1.93	
	Air	1.14	0.76	
	Total	**6.52**	**5.13**	**5.07**
	Cooling water [b]	21.04	15.9	
OUTPUT	Hot metal	1	1	1.05 (4.5% C)
	Slag	0.18	0.167	0.21
	Condensed water vapor in slurry	0.84	0.64	
	Hot water not used	1.823	1.66	
	Steam not used	0.59	0.15	
	Total discharged gas	2.08	1.51	3.81
	Carbon dioxide	0.99[e]	0.98[e]	1.60[c]
	Nitrogen	0.89	0.59	2.21
	Total[d]	**6.52**	**5.13**	**5.07**
	Cooling water in slurry	21.04	15.9	
	Carbon dioxide from $CaCO_3$ and $MgCO_3$ calcination	0.04	0.04	

a. All BF ironmaking process data were from Pinegar, et al.[13-14]
b. The cooling water was used for off-gas cleaning and water vapor condensation in suspension process.
c. This data did not include the carbon dioxide emission from ore/coke preparation.
d. If the temperature of molten iron and slag is 1600 ˚C, the total material consumption will be 7.08 and 5.63 t/tHI for one-step and two-step respectively.
e. This data did not include CO_2 from calcinating $CaCO_3$, $MgCO_3$.

Table 5.4. Energy balance for the reformerless suspension ironmaking process with natural gas, GJ/tHI

Items		1-step Process	2-step Process	BF Process[a]
INPUT	Fuel combustion[b]	13.66	9.72	8.33
	Heat recovery	-5.03	-2.47	-1.32
	Waste heat boiler	-3.43	-2.07	
	Steam not used[c]	-1.58	-0.4	
	Subtotal	8.65	7.25	7.01
	Energy input for ore/coke preparation			5.68
	Total	**8.65**	**7.25**	**12.7**
	Energy input for $CaCO_3$ and $MgCO_3$ calcination	0.26[d]	0.26[d]	
OUTPUT	Reduction	0.92	0.91	2.1
	Sensible heat of hot iron	1.27 (1500°C)	1.27 (1500°C)	1.35 (1600°C)
	Sensible heat of slag	0.29 (1500°C)	0.29 (1500°C)	0.47 (1600°C)
	Slurry (H_2O(l))	2.28 (50°C)	1.73 (50°C)	
	Hot water not used	1.53 (220°C)	1.39 (220°C)	
	Exhausted gas	0.66 (300°C)	0.47 (300°C)	0.26 (90°C)

Table 5.4 Continued

OUTPUT	$CaCO_3$ decomposition			0.33
	Slag forming			-0.17
	Heat loss in the reactor(s)	0.8	0.8	2.6
	Heat loss in the heat exchangers	0.74[e]	0.35[e]	0.07
	Steam not used (90^oC)[c]	0.16	0.04	
	Subtotal	8.65	7.25	7.01
	Pelletizing			3.01
	Sintering			0.65
	Cokemaking			2.02
	Total[f]	**8.65**	**7.25**	**12.7**
	$CaCO_3$ and $MgCO_3$ calcination at 1000^oC	0.26	0.26	

a. All BF ironmaking process data were from Pinegar, et al. [13-14]. In which energy balance was calculated by METSIM based on the material balance and at operating temperature of 1600˚C.
b. Fuel combustion energy was calculated by subtracting the energy used for iron ore reduction from the balance of heats of formation of all output components from the entire system and input components into it [13] The higher heating value of natural gas was used for this calculation. If lower heating value is used, total energy requirements for the one-step and two-step processes will decrease to 4.85 and 4.41 GJ/tHI respectively.
c. Energy recovered by steam not used in the process consists of energy from steam condensation and the sensible heat of steam from 300 to 90˚C.
d. Energy needed for calcinating flux ($CaCO_3$ and $MgCO_3$) to generate CaO and MgO was calculated by METSIM at 1000 ˚C.
e. Heat losses in a heat exchanger were assumed to be 5% of the total sensible heat of input streams.
f. If the temperature of molten iron and slag is 1600˚C, total energy requirements for the one-step and two-step processes will be, respectively, 9.43 and 7.87 GJ/tHI using high heating value.

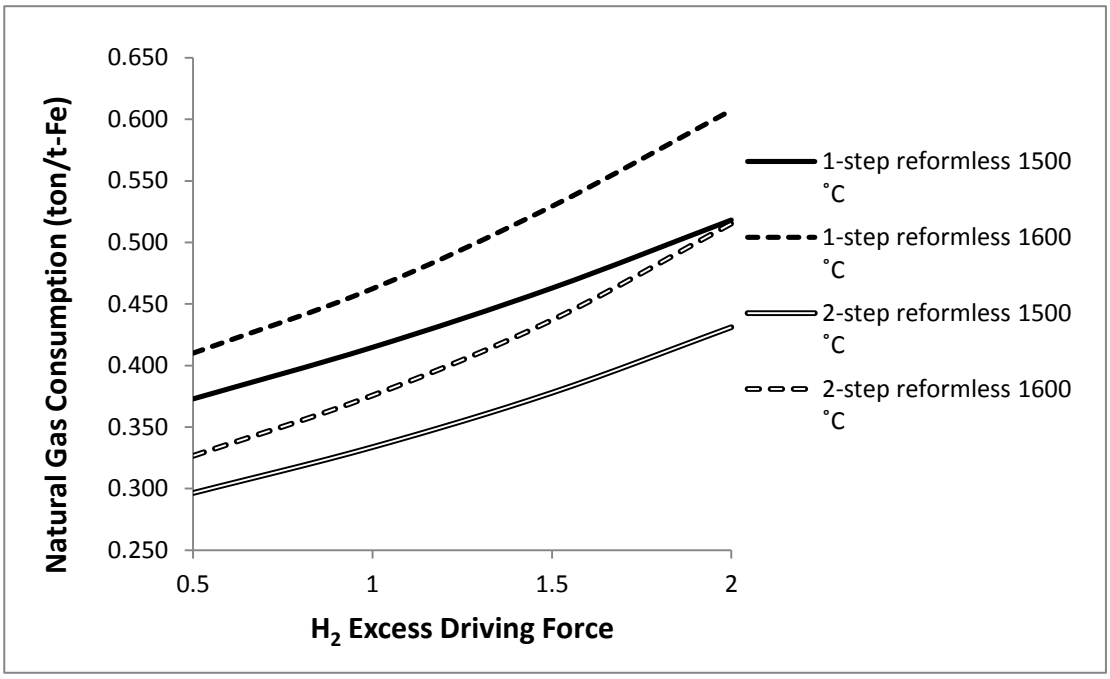

Figure 5.4. Effect of H_2 excess driving force on natural gas consumption rate in reformerless suspension ironmaking process

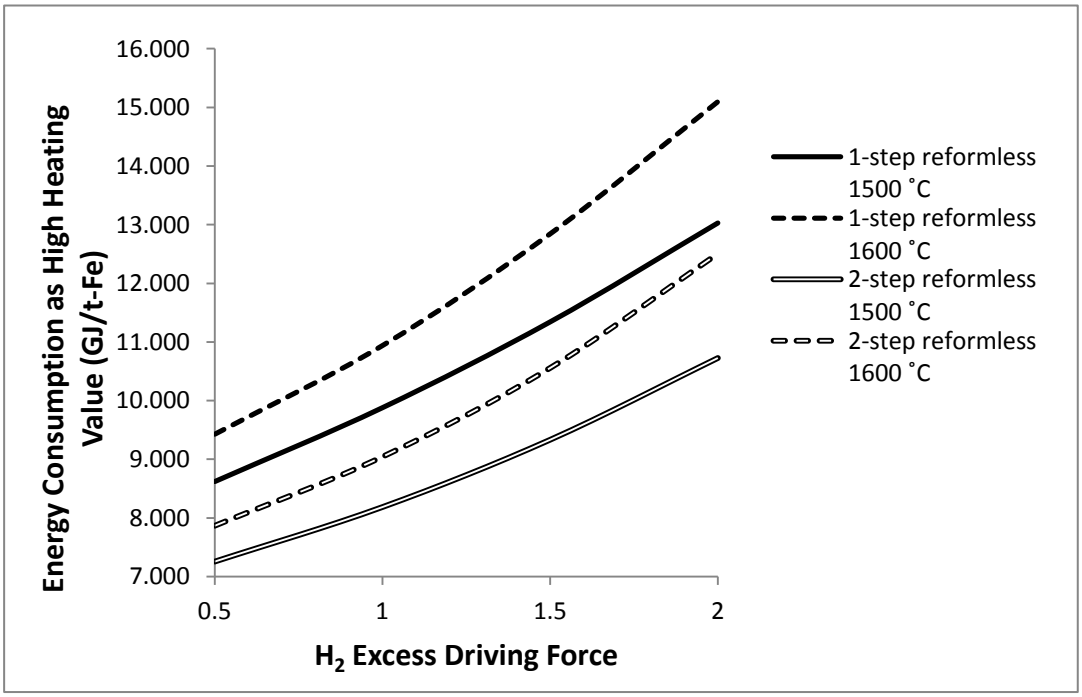

Figure 5.5. Effect of H_2 excess driving force on energy consumption in reformerless suspension ironmaking process

and one-step SMR-syngas emits 31% and 28% less CO_2 than cited blast furnace ironmaking process, respectively; (2) energy consumption in the suspension ironmaking process with one-step SMR-H_2 and one-step SMR-syngas is a little higher than is the cited ironmaking process.

5.4. Comparison of Simulated Suspension Ironmaking Processes

Main parameters for the one-step suspension ironmaking processes with different H_2 sources at the base conditions of simulation are summarized in Table 5.7. It can be seen that besides the suspension ironmaking process with pure H_2, the reformerless suspension ironmaking process with natural gas consumes the least fuel, emits the least CO_2 and has the least energy consumption. Therefore, the reformerless suspension ironmaking process with natural gas is the most competitive one if cheap H_2 is not available. Compared to the cited blast furnace ironmaking process, the one-step reformerless suspension ironmaking process with natural gas emits 36% less CO_2 and consumes 30% less energy than the cited blast furnace ironmaking process.

Comparison of simulation results of this study to those of Pinegar et al. is shown in Table 5.8. It can be seen that FeO activity coefficient in slag has considerable effect on mass and energy balances of the suspension ironmaking process. Compared to the simulation results of Pinegar et al., the following differences were found in this study:

(1) for the pure H_2 process, H_2 and energy consumption increased 10% and 14%, respectively.

(2) for the reformerless process, natural gas and energy consumption is almost the same due to excess O_2 in the offgas of burner decreased from 5% to about 0.8%.

Table 5.5. Material balance of the suspension ironmaking process with SMR-H_2 and SMR-syngas, ton/tHI

Item		SMR-H_2	SMR-syngas	BF Process[a]
INPUT	**Ironmaking**			
	Hydrogen	0.12		
	Syngas		0.83	
	Oxygen	0.44	0.58	
	Syngas		0.84	
	Iron ore	1.5 (magnetite)	1.5 (magnetite)	1.43 (hematite)
	Flux	0.06	0.06	0.29
	Air			2.89
	Coke			0.46
	Total Ironmaking	**2.12**	**2.98**	**5.07**
	SMR-H_2 or SMR-Syngas			
	Natural gas	0.4	0.42	
	Air	3.17	2.93	
	PSA tail gas from ironmaking	0.02	0.73	
	Fresh water for steammaking	2.15	2.48	
	Total SMR	**5.74**	**6.56**	
	Total material input	**7.86**	**9.54**	**5.07**
	Cooling water for scrubber	18.07	20.05	

Table 5.5 Continued

OUTPUT	**Ironmaking**			
	Hot iron	1	1	1.05 (4.5% C)
	Slag	0.17	0.17	0.21
	Condensed water vapor	0.93	1.08	
	Total discharged gas	0.02	0.73	3.81
	Total-Ironmaking	**2.12**	**2.98**	**5.07**
	CO_2	1.06[b]	1.11[c]	1.60[d]
	Carbon dioxide from $CaCO_3$ and $MgCO_3$ calcination	0.04	0.04	
	SMR - H_2 or SMR-Syngas			
	Hydrogen	0.12		
	Syngas		0.85	
	Flue gas	4.06	3.7	
	Hot water not used	0.82	1.25	
	Steam not used	0.74	0.76	
	Total SMR	**5.74**	**6.56**	
	Total material output [e]	**7.86**	**9.54**	**5.07**

a. All BF ironmaking process data were from Pinegar et al.[13-14], in which energy balance was calculated by METSIM based on the material balance and at operating temperature of 1600˚C.
b. Total CO_2 of ironmaking process and SMR-H_2 process .
c. Total CO_2 of ironmaking process and SMR-syngas process .
d. Carbon dioxide emission from ore/coke preparation was not included in this data.
e. If the temperature of molten iron and slag is 1600 ˚C, the total material consumption is 8.45 and 10.54 ton/tHI for SMR-H_2 and SMR-syngas respectively.

Table 5.6. Energy balance of suspension ironmaking process with SMR-H_2 and SMR-syngas, GJ/tHI

Items		SMR – H_2	SMR – syngas	BF Process[a]
INPUT	**Ironmaking**			
	Fuel combustion[b]	8.93	10.41	8.33
	Produced hydrogen	0.01 (30°C)		
	Produced syngas		0.01 (30°C)	
	Heat recovery	-2.8	-3.7	-1.32
	Subtotal	6.14	6.72	7.01
	Energy input for ore/coke preparation			5.68
	Total-Ironmaking	**6.13**	**6.72**	**12.7**
	Energy input for $CaCO_3$ and $MgCO_3$ calcination	0.26[c]	0.26[c]	
	SMR-H_2 or SMR-Syngas			
	Fuel combustion[b]	8.72	9.05	
	Sensible heat from feed gases	0.01	0.005	
	Steam not used[d]	-1.99	-2.06	
	Total-SMR	**6.74**	**7**	
	Total high heating value energy input[e]	**12.88**	**13.72**	**12.7**
OUTPUT	**Ironmaking**			
	Reduction	0.92	0.92	2.09
	Slagmaking			-0.16
	Sensible heat of hot iron	1.27 (1500°C)	1.27 (1500°C)	1.35 (1600°C)
	Sensible heat of slag	0.29	0.29	0.47
	Slurry (H2O(l))	1.96 (1500°C)	2.17 (1500°C)	
	Condensed water vapor after scrubber	0.004	0.006	
	Sensible heat of offgas			0.26 (90°C)
	$CaCO_3$ decomposition			0.33

Table 5.6 Continued

OUTPUT	PSA tail gas	0.001	0.005	
	Heat loss in the reactor	0.8	0.8	2.6
	Heat loss in heat exchanger	0.35[f]	0.46[f]	0.07 (heat loss in heat recovery)
	Heat loss after the scrubber	0.55	0.8	
	Pelletizing			3.01
	Sintering			0.65
	Cokemaking			2.02
	Total-Ironmaking	**6.14**	**6.72**	**12.7**
	$CaCO_3$ and $MgCO_3$ decomposition at 1000°C	0.26	0.26	
	SMR-H_2 or SMR-Syngas			
	Steam-methane reforming	3.45	3.58	
	Produced hydrogen	0.009 (30°C)		
	Produced syngas		0.01	
	Flue gas	1.33 (300°C)	1.17 (300°C)	
	Hot water not used	0.69	1.04	
	Heat loss in the reformer	1.06	0.99	
	Steam not used (90°C)[d]	0.2	0.21	
	Total-SMR	**6.74**	**7**	
	Total high heating value energy output	**12.88**	**13.72**	**12.7**

a. All BF ironmaking process data are from journals of Pinegar et al.[13-14], in which energy balance was calculated by METSIM based on the material balance and at operating temperature of 1600˚C.
b. Fuel combustion energy was calculated by subtracting the energy used for reforming from the balance of heats of formation of all output components from the SMR section and input components into it [14]. The high heating value of natural gas was used for this calculation. If the low heating value is used, the total energy requirements for the ironmaking section will be 3.87 GJ and 4.08GJ/ton of hot iron, respectively.
c. The energy needed for $CaCO_3$ and $MgCO_3$ calcination to generate CaO and MgO was calculated by METSIM. Calcination was assumed to be done at 1000°C which was separately from the ironmaking process[14].
d. Heat losses in a heat exchanger were assumed to be 5% of the total sensible heat of input streams.
e. If temperature of molten iron and slag is 1600°C, the total energy consumption will be 13.93 and 15.22 GJ/tHI for SMR-H_2 and SMR-syngas respectively.

Table 5.7. Comparison of one-step suspension ironmaking processes with different H_2 sources

Item	Pure H_2	Reformerless	SMR - H_2	SMR - syngas	BF[e]
Coke, t/tHI					0.462
H_2, t/ tHI	0.107				
Natural gas, t/ tHI		0.37	0.4	0.42	
CO_2 emission, t/ tHI	0.04[a]	1.03[a]	1.10[a]	1.15[a]	1.60[b]
Energy[c] (GJ/ tHI)	6.53	8.91	13.14	13.98	12.7

a. CO_2 emission from flux calcination was included.
b. CO_2 emission from ore/coke preparation is not included.
c. BF energy consumption includes energy for ore/coke preparation and iron making. Suspension ironmaking energy include energy requirement for flux calcination.
e. All BF ironmaking process data were from Pinegar et al. [13-14].

Table 5.8. Comparison of this study with of Pinegar's under base conditions.

Process	Comparison	%FeO	β	Mass[a] Mt/tHI	HHV Energy[b] GJ/tHI	H_2 Mt/tHI	Natural Gas Mt/tHI	CO_2[c] Mt/tHI
	Pinegar et al.[15]	9.64	0.990	2.09	5.74	0.1		0.04
	This study	26.05	0.967	2.17	6.53	0.11		0.04
Pure H_2	Change %	170	-2	4	14	10		0
	Pinegar et al.[13]	9.64	0.990	6.93	8.94		0.37	1.02
	This study	26.05	0.967	6.56	8.91		0.37	1.03
Reformerless	Change %	170	-2	-5	0		0	1
	Pinegar et al.[14]	9.64	0.990	8.84	12.96		0.39	1.08
	This study	26.05	0.967	7.9	13.14		0.4	1.1
SMR-H_2	Change %	170	-2	-11	1		3	2
	Pinegar et al.[14]	9.64	0.990	10.35	13.76		0.41	1.15
	This study	26.05	0.967	9.58	13.98		0.42	1.15
SMR-syngas	Change %	170	-2	-7	2		2	0

a. Fluxes in this table are limestone and dolomite.
b. Energy required for limestone and dolomite calcinations is included
c. CO_2 from flux calcination is included.

(3) because of the same reason as (2), for the SMR-H_2 process, the consumption of energy and natural gas slightly increased by 1% and 3%, respectively, and for the SMR-syngas process, the consumption of energy and natural gas both increased by 2%.

CHAPTER 6

ECONOMIC ANALYSIS OF THE SUSPENSION IRONMAKING PROCESS

6.1. Economic Indices

The following four indices were used for analyzing the economic feasibility of the suspension ironmaking process: net present value (NPV), capital cost, operating cost and CO_2 credit. In this research, the same method and procedure to calculate these indices as those of Pinegar et al. were adopted [16].

NPV is defined as

$$(NPV) = \sum_{i=0}^{n} \frac{C_i}{(1+r)^i}, \tag{6.1}$$

where C_i is cash flow in the end of the *ith* year, r is the discount rate and n is the number of years the project spans.

The NPV was estimated based on pure H_2 and natural gas under the base simulation conditions (see Table 4.1). Assume the project would span 15 years and the discount rate would be 10%. Capital investment was assumed to be spent equally at the

beginning of the project and the end of year one. It was also assumed that the plant starts at the beginning of year two in full production. The total net annual cash flow was calculated by the balance of inflow (hot iron, electricity generated, and CO_2 emission credit) and outflow (operating cost). The hot iron price was \$512/ton [32] in 2010 dollar value.

The following standard scaling-up equation for calculating capital cost was used in this research [15-16]

$$\textit{(Capital cost of scaled up plant)} = \textit{(Base capital cost)} \times \left(\frac{\textit{Scaled up production rate}}{\textit{Base production rate}} \right)^{0.6} \tag{6.2}$$

Values of base capital costs and base production rates were found from the literature by Pinegar et al. [16], and were summarized under the "Base" column in Table 6.1. Since most base costs were in pre-2010 dollar value, the capital cost calculated by equation (4.1) was further converted to 2010 dollar values by using Chemical Engineering Plant Cost Index (CEPCI) in the following equation[33]:

$$\textit{(Capital cost of plant at present time)} = \textit{(capital cost at the time of the reference)} \times \left(\frac{\text{CEPCI}\ \textit{at present time}}{\text{CEPCI}\ \textit{at the time of the reference}} \right) \tag{6.3}$$

Table 6.1. Capital cost of a suspension ironmaking plant with different H_2 sources in 2010 dollar values

Section		Base	1-step Pure H_2	2-step Pure H_2	1-step Reformerless	2-step Reformerless	1-step SMR-H_2	1-step SMR-syngas
Ironmaking	Capacity, Million t/year	0.5	1.0	1.0	1.0	1.0	1.0	1.0
	Year	1994	2010	2010	2010	2010	2010	2010
	Capital Cost, $ Million	194	298	466	298	466	327	330
Power Generation	Capacity, MW	108.9	40.3	9.7	45.3	11.6	37.0	48.9
	Year	1998	2010	2010	2010	2010	2010	2010
	Capital Cost, $ Million	54.4	45.0	19.0	49.0	22.0	43.0	51.0
Hydrogen Recycle	Capital Cost, $ Million				67	49		
Heat Exchanger	Capacity, Kg H_2/h	3,669			22,473	14,775		
	Year	2004			2010	2010		
	Capital Cost, $ Million	1			4	3		
WGS Reactor	Capacity, Kg H_2/h	3,669			22,473	14,775		
	Year	2004			2010	2010		
	Capital Cost, $ Million	3			12	9		
PSA	Capacity, Kg H_2/h	3,669			22,473	14,775		
	Year	2004			2010	2010		
	Capital Cost, $ Million	8			32	24		
Boiler I	Capacity, Kg Steam/h	51,5097			65,348	45,308		
	Year	1998			2010	2010		
	Capital Cost, $ Million	17.2			7.0	6.0		
Boiler II	Capacity, Kg Steam/h	51,5097			141,199	61,833		
	Year	1998			2010	2010		
	Capital Cost, $ Million	17.2			12.0	7.0		
Hydrogen Production	Capacity, Kg H_2/day	135,000					399,885	415,028
	Year	2002					2010	2010
	Capital Cost, $ Million	62.8					179	182
Total Capital Cost, $ Million			**343**	**485**	**414**	**537**	**549**	**563**

In this calculation, CEPCI of 2010 [34] was set to be the present time.

Operating cost consists of material and nonmaterial operating costs. The material cost includes the cost of iron ore concentrate, flux, fuel and oxygen, while nonmaterial cost includes labor, maintenance and electricity. In this study, the same methods as those of Pinegar et al. [16] were adopted to estimate both material cost and nonmaterial cost. The base price and the calculated operating cost for all of the simulation processes are summarized in Table 6.2.

CO_2 credit was calculated by multiplying potential trading price of CO_2 emissions with the difference of CO_2 emission levels between blast furnace ironmaking process and the suspension ironmaking process, based on the concept of "cap and trade system for greenhouse gas," which was discussed by Pinegar et al. [16].

6.2. Results of Economic Analysis

Table 6.1 shows the calculated results for capital cost of one million ton suspension ironmaking plant with different H_2 sources in 2010 dollar values. It can be seen that (1) total capital cost changes from 343 million dollars with one-step pure H_2 to 560 million dollars with one-step SMR-syngas; (2) SMR technology is still very expensive, resulting in very high capital cost for the suspension ironmaking plant combined with built-in SMR sections; (3) a one-step natural gas reformerless suspension ironmaking plant requires 414 million dollar capital cost, which could be the most promising option except the pure H_2 process.

Calculated results of operating cost of a suspension ironmaking plant with different H_2 sources are listed in Table 6.2. One can see that suspension ironmaking process with

Table 6.2. Operating cost of a suspension ironmaking plant with different H_2 sources, $/tHI

Item	Reference Price	1-step H_2	2-step H_2	1-step Reformerless	2-step Reformerless	1-step SMR-H_2	1-step SMR-syngas
Hydrogen	$2.5/kg [16]	267	222				
Natural gas	$254/ton [16]			95	75	101	106
Industrial O_2	$0.08/$Nm^3$ [16]	26	18	45	33	25	32
Iron ore concentrate	$167/ton [16]	250	250	250	250	250	250
Flux	$105/ton [35]	6	6	6	6	6	6
Ironmaking operating cost [16]		26	52	26	52	26	52
Labor [16]		2	4	2	4	2	2
Maintenance [16]		15	30	15	30	15	15
Electricity [16]		9	18	9	18	9	9
SMR-H2 or SMR -syngas Operating Cost [16]						17	19
Power generation operating cost	$20/MWh [16]	6	1	7	2	5	7
Total Operating Cost		**581**	**549**	**429**	**418**	**430**	**446**

pure H_2 has the highest operating cost, and with reformerless natural gas has the lowest operating cost. Therefore, from the operating cost point of view, the reformerless suspension ironmaking process with natural gas appears the most promising.

Assume the potential trading price of CO_2 emission is $50/t. CO_2 credit was calculated and is tabulated in Table 6.3. It can be seen that the suspension ironmaking process with pure H_2 receives the largest credit, with the reformerless natural gas next, and SMR-syngas the least.

Table 6.3. CO_2 credit for suspension ironmaking plant with different H_2 sources under base conditions by assuming \$50 /t CO_2.

Item	1-step Pure H_2	2-step Pure H_2	1-step Natural Gas Reformerless	2-step Natural Gas Reformerless	1-step SMR-H_2	1-step SMR-syngas	BF*
CO_2 Emission, t/tHI	0.04	0.04	1.03	0.83	1.1	1.15	1.724
CO_2 Credit, \$/tHI	84.2	84.2	34.7	44.7	31.2	28.7	0

* Average CO_2 emission from BF and from ore/coke preparation.

Calculated net present values for the suspension ironmaking plant with different H_2 sources are listed in Table 6.4. From this table, one can see that (1) with no or small CO_2 credit, suspension ironmaking process with pure H_2 is not economical, largely due to high H_2 cost, but when CO_2 credit is large, such as \$100/t CO_2 emission, the process could turn out to be economical; (2) of all processes considered, the reformerless suspension ironmaking process with natural gas is the most profitable and always economical regardless of large or small CO_2 credit; (3) the one-step reformerless suspension ironmaking process with natural gas is more profitable than the two-step suspension ironmaking process since the two-step requires much higher capital investment.

6.3. Sensitivity Analysis

In sensitivity analysis of economics, four parameters are considered, H_2 price, operating cost, hot iron price and CO_2 credit. The base conditions are price of H_2 \$2.5/kg, price of natural gas \$254/ton, operating cost in Table 5.2, and CO_2 credit \$0/tHI.

Table 6.4. NPV for suspension ironmaking plant with different H_2 sources under base conditions

Item		1-step Pure H_2	2-step Pure H_2	1-step Natural Gas Reformerless	2-step Natural Gas Reformerless	1-step SMR-H_2	1-step SMR-syngas
Capital Cost, $ MM		343	485	414	537	549	563
Operating Cost, $/tHI		581	549	429	418	430	446
NPV, $MM	$0/ton CO_2 emission	-667	-686	333	177	168	84
	$50/ton CO_2 emission	-85	-104	573	486	384	282
	$100/ton CO_2 emission	497	479	813	795	599	480

Effects of deviation of these parameters from base conditions on net present values were calculated and the results are shown in Appendix E.

For the suspension ironmaking process with pure H_2, a decrease of H_2 price and operating cost and an increase of the hot iron price and CO_2 credit can improve economic feasibility of the process. However, reduction of H_2 price alone does not improve very much the economic feasibility, mainly due to a very high present H_2 price. When the CO_2 emission price rises very high, such as greater than $100/ton, the suspension ironmaking process will be economically feasible.

For the reformerless suspension ironmaking process with natural gas, it is economically feasible in the base case. Deviation of natural gas price does not affect the economical feasibility of the process as seriously as H_2 price does. Larger CO_2 credit could make the process even more economical. Reduction of total operating cost and increase of hot iron price would definitely make the process more competent.

Suspension ironmaking processes with SMR-H_2 and SMR-sysgas are more economical than with pure H_2, but less than with reformerless natural gas.

CHAPTER 7

SUMMARY AND CONCLUSIONS

Process simulation and economic analysis with a Metsim simulation software package for the novel suspension ironmaking process with consideration of the activity coefficient of FeO in slag have been studied in this thesis. Models in the literature for calculating the activity coefficient of FeO in slag were chosen in the first place. Square Root of Mean Sum of Squares of Differences (SRMSSD) between the predicted and measured values of activity coefficients of FeO in slag was used as the criterion for choosing the most appropriate model to be used in this study. Hundreds of experimental data of activity coefficient of FeO in slag from the literature were collected, reviewed and assessed. Sixteen of them[23, 28, 30] were utilized to evaluate the models of the activity coefficient of FeO in slag since their experimental conditions were closer to the conditions of the suspension ironmaking process. Of all models evaluated, Park and Lee's regular solution model [27] gave the smallest value of SRMSSD and was selected to calculate the activity coefficient of FeO in slag in this simulation study.

With different H_2 sources, six suspension ironmaking processes, one-step pure H_2, two-step pure H_2, one-step reformerless natural gas, two-step reformerless natural gas, one-step SMR-H_2, and one-step SMR-syngas, were simulated. Flow diagrams of these suspension ironmaking processes were first created, and then translated into Metsim

block diagrams. Park and Lee's FeO activity coefficient model [27] was integrated with Metsim the simulation model. A one-million ton hot iron per year suspension ironmaking plant was simulated for material balance, energy balance and CO_2 credit.

The simulation results show that compared to the average conventional blast furnace ironmaking process, the suspension ironmaking process would emit considerably less CO_2. Processes of pure H_2 and reformerless natural gas are more energy efficient, but SMR-H_2 and SMR-syngas are less energy efficient than the blast furnace ironmaking process. The suspension iromaking process can directly use iron ore concentrate and does not need coke whereas for conventional blast furnace ironmaking process requires on agglomeration of iron ore and fuel, such as sintering, pelletization and cokemaking. Directly using iron ore concentrate is one of the principal reasons why the suspension ironmaking process is more energy efficient. However, due to the requirement of H_2 as fuel and reducing agent, the source of H_2 becomes a dominant factor affecting energy consumption and economics of the suspension ironmaking process. The simulation results show that if excluding the pure H_2 process, the reformerless natural gas process is the most energy-efficient, and it consumes 30-41% less energy than the average conventional blast furnace ironmaking process.

Four economical indices were adopted in this study to evaluate the economical feasibility of the suspension ironmaking process: capital cost, operating cost, CO_2 credit and net present value. The pure H_2 process is very energy efficient and receives the largest CO_2 credit of all suspension ironmaking processes simulated. The capital cost for a one-million ton hot iron per year plant is $343 million for the one-step pure H_2 suspension ironmaking process and $485 million for the two-step pure H_2 suspension

ironmaking process. The pure H_2 suspension ironmaking process will become economical when H_2 price decreases or CO_2 credit increases greatly.

Of all suspension ironmaking processes simulated, the reformerless natural gas process is the most profitable. The capital costs for a one million ton per year one-step reformerless suspension ironmaking plant with natural gas is $414 million and for two-step is $537 million. The operating cost are $429/tHI and $418/tHI for one-step and two-step reformerless natural gas processes, respectively. Without considering CO_2 credit, net present value is $333/tHI and $177/tHI for one-step and two-step, respectively, but if taking $100/t CO_2 credit, the NPV will jump to $813/tHI and $795/tHI, respectively.

The SMR-H_2 and SMR-syngas processes are also profitable even under the current conditions without considering CO_2 credit though their capital cost is higher.

APPENDIX A

METSIM PROCESS SIMULATION BLOCK DIAGRAMS

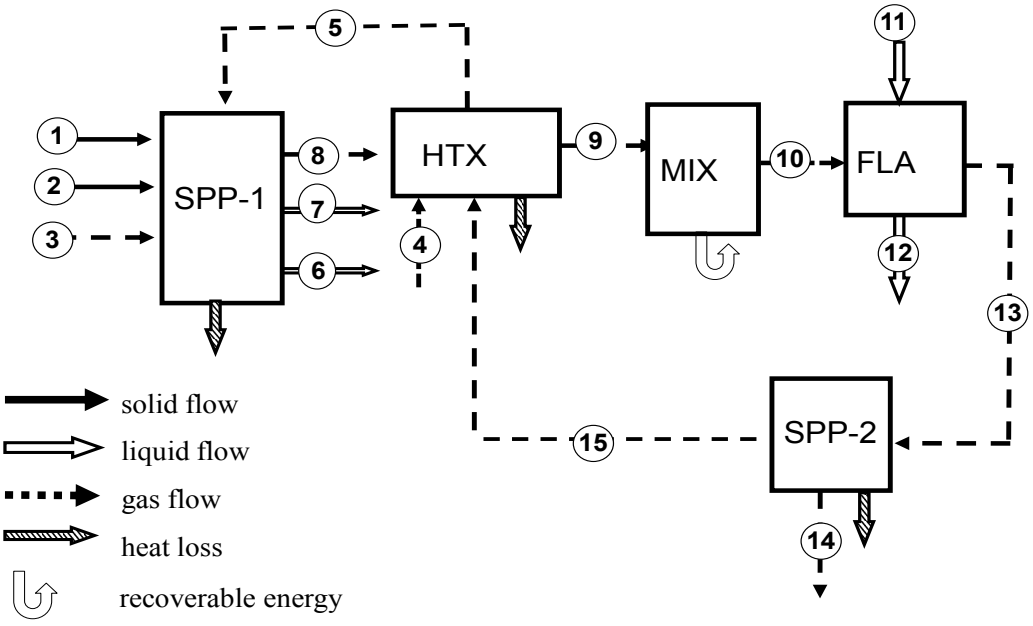

Figure A.1. Block diagram for simulation of one-step suspension ironmaking process with pure H_2

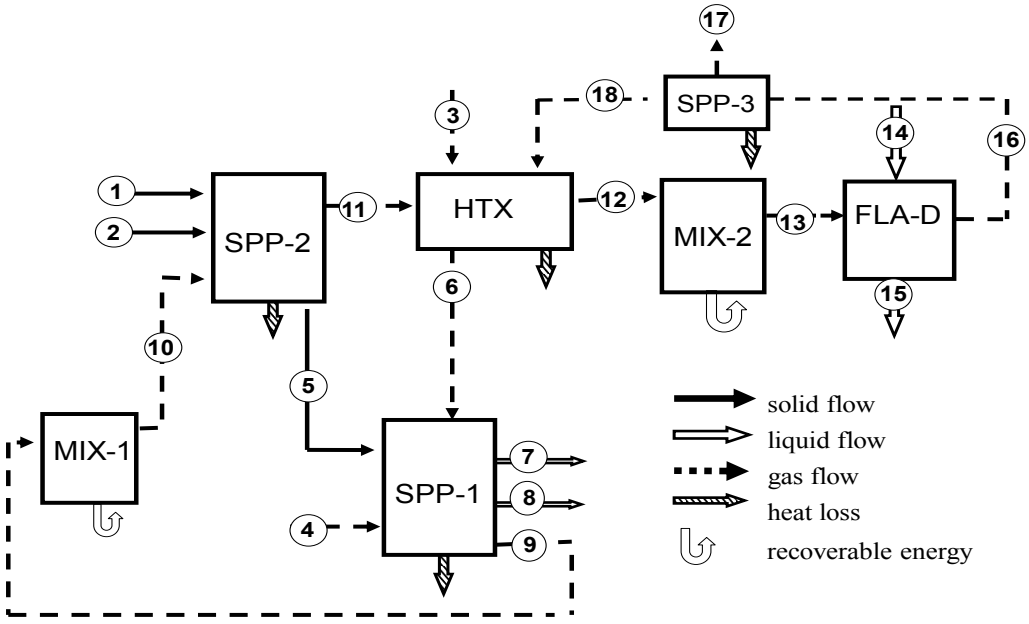

Figure A.2. Block diagram for simulation of two-step suspension ironmaking process with pure H_2

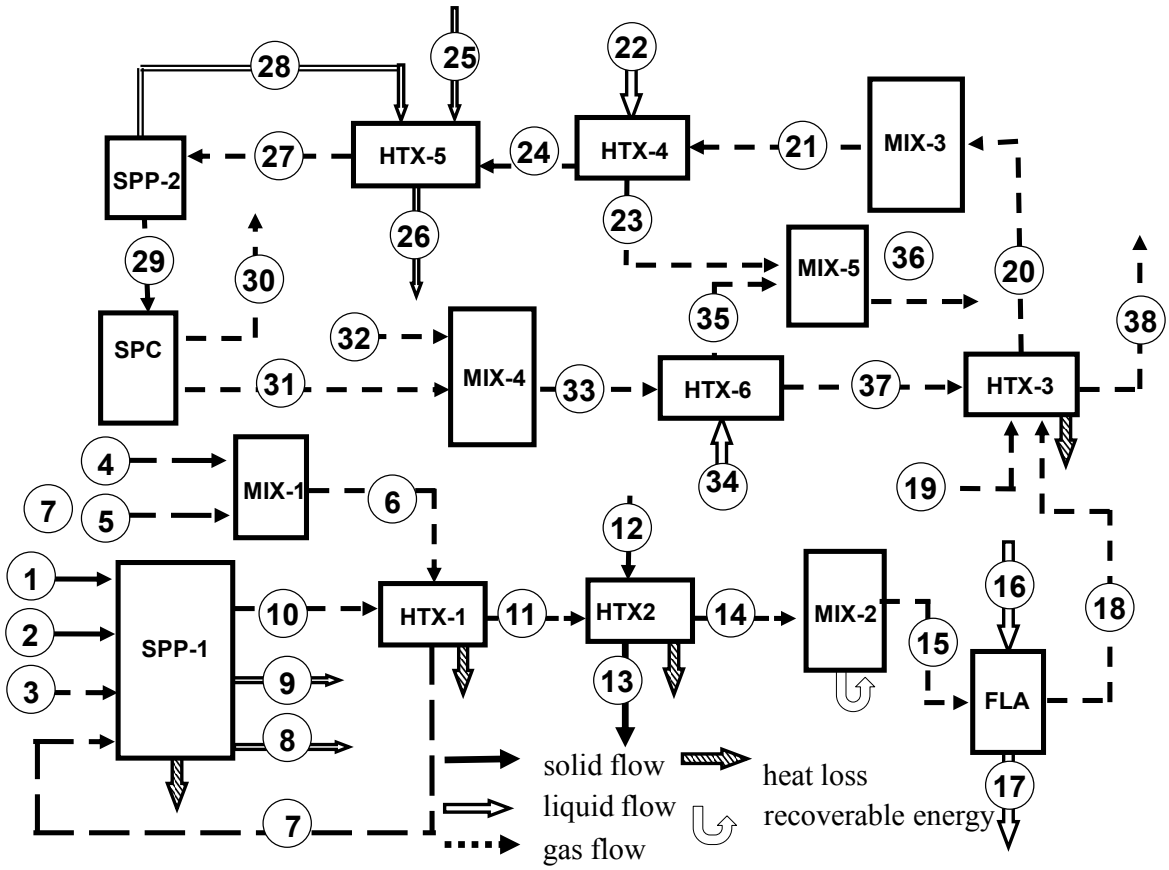

Figure A.3. Block diagram for simulation of one-step reformerless suspension ironmaking process with natural gas

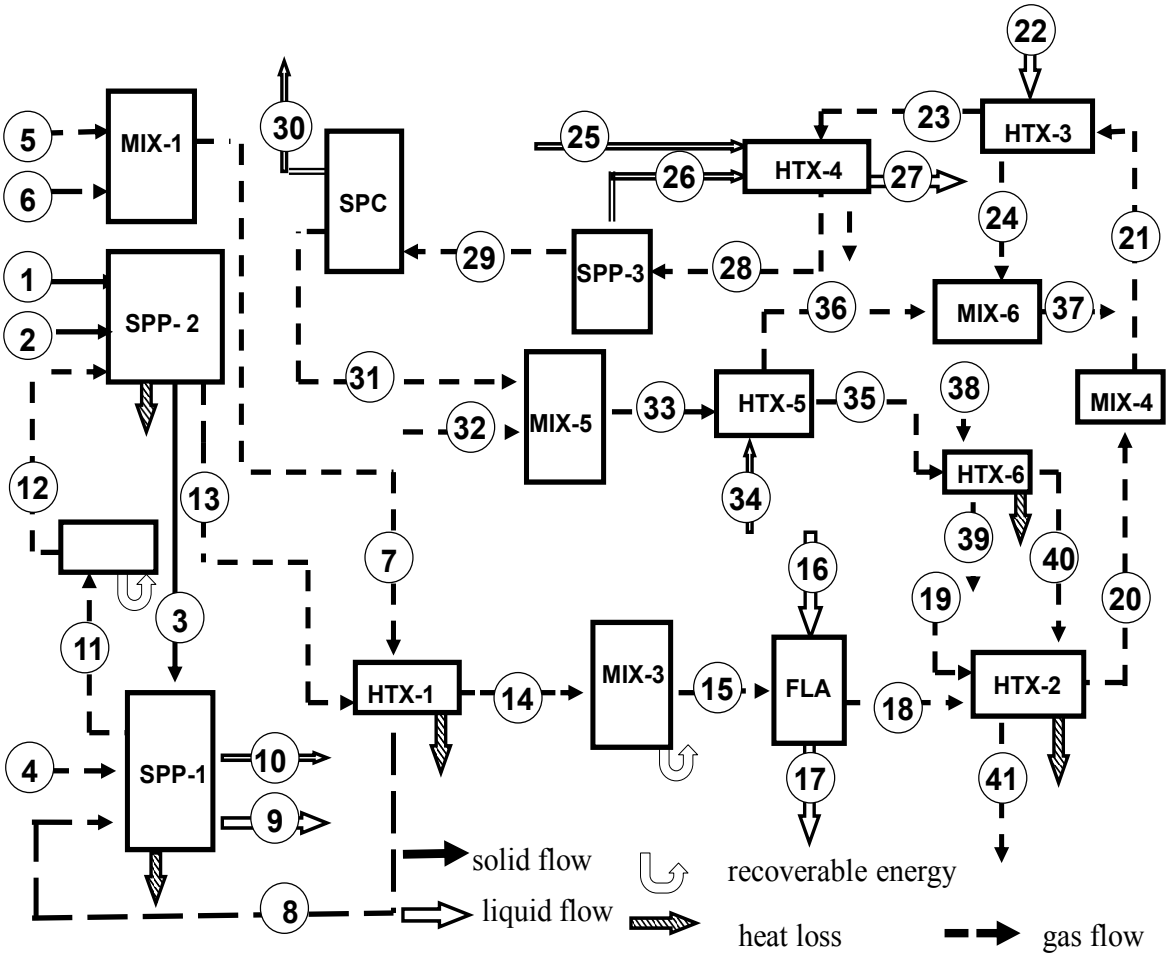

Figure A.4. Block diagram for simulation of two-step reformerless suspension ironmaking process with natural gas

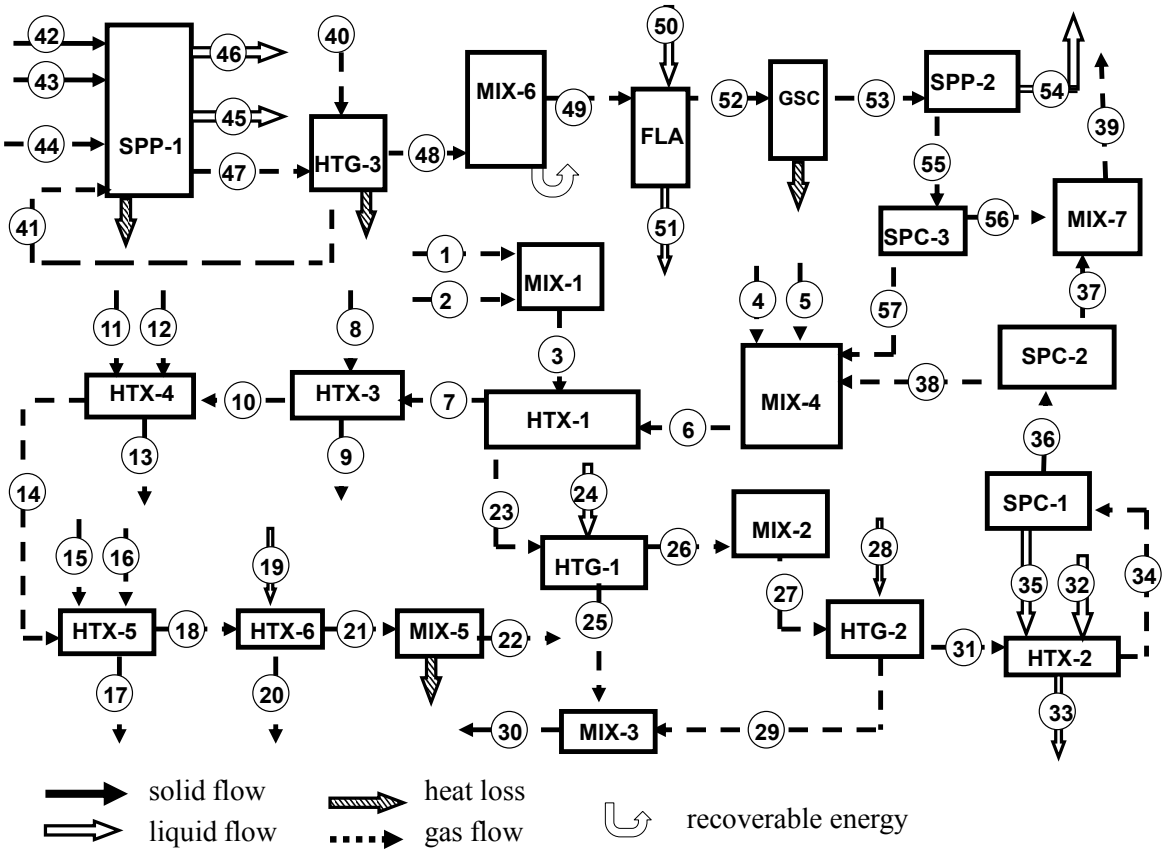

Figure A.5. Block diagram for simulation of one-step suspension ironmaking process with SMR-H_2

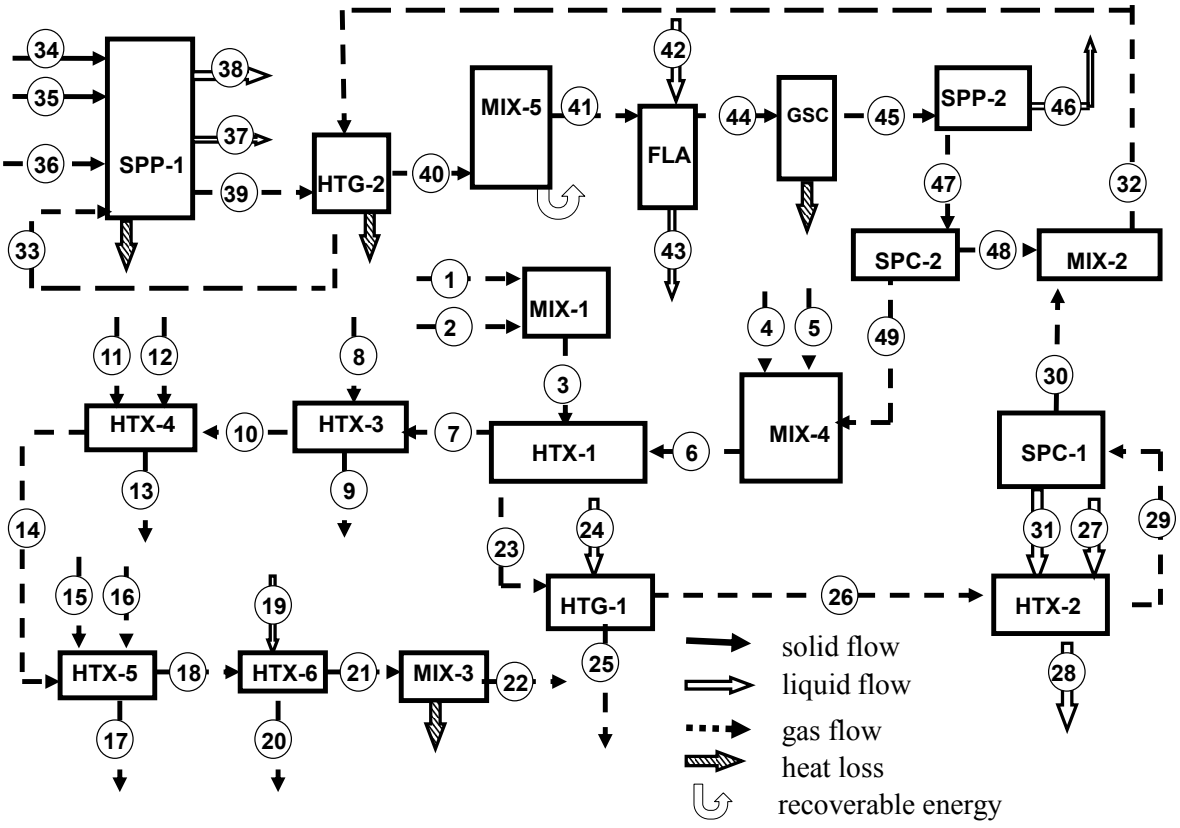

Figure A.6. Block diagram for simulation of one-step suspension ironmaking process with SMR-syngas

APPENDIX B

DESCRIPTION OF UNITS IN SIMULATION

BLOCK DIAGRAMS

Table B.1. Description of units in Figure A.1 for simulation of one-step suspension ironmaking process with pure H_2

Unit	Description
SPP-1	Ironmaking reactor
HTX	H_2 heater in which H_2 was heated by sensible heat of off-gas from ironmaking reactor
MIX	Waste heat boiler used to recover sensible heat of off-gas from heat exchanger.
FLA	Scrubber used to clean gas and condense water vapor in offgas.
SPP-2	Water remover to remove water vapor from clean gas

Table B.2. Description of units in Figure A.2 for simulation of two-step suspension ironmaking process with pure H_2

Unit	Description
SPP-1	Ironmaking reactor in which wustite was reduced to molten iron.
SPP-2	Iron ore prereducing reactor in which iron ore concentrate was reduced to solidus wustite.
HTX	H_2 heater in which H_2 was heated by sensible heat of off-gas from ironmaking reactor
MIX-1	High temperature waste heat boiler used to recover sensible heat of off-gas from ironmaking reactor.
MIX-2	Waste heat boiler used to recover sensible heat of off-gas from heat exchanger.
FLA	Scrubber used to clean gas and condensed water vapor in the gas.
SPP-3	Water remover .

Table B.3. Description of units in Figure A.3 for simulation of one-step reformerless suspension ironmaking process with natural gas

Unit	Description	Unit	Description
SPP-1	Ironmaking reactor	HTX-4	Steam boiler
MIX-1	Natural gas and steam mixer	HTX-5	Overheated water boiler
HTX-1	Feed gas (natural gas and steam) preheater	SPP-2	Water remover
HTX-2	Natural gas heater	SPC	Pressure swing adsorption (PSA)
MIX-2	Waste heat boiler to extract recoverable energy after two heat exchangers.	MIX-4	PSA off-gas burner
FLA	Scrubber used to clean gas and condense water vapor in the gas.	HTX-6	Steam boiler2
HTX-3	Feed gas preheater of water gas shift reactor	MIX-5	Steam mixer
MIX-3	Water gas shift reactor		

Table B.4. Description of units in Figure A.4 for simulation of two-step reformerless suspension ironmaking process with natural gas

Unit	Description	Unit	Description
SPP-1	Ironmaking reactor in which wustite was reduced to molten iron.	HTX -3	Steam boiler 1
SPP-2	Iron ore pre-reducing reactor in which iron ore concentrate was reduced to solidus wustite.	HTX -4	Overheated water boiler
MIX-1	Natural gas and steam mixer	SPP-3	Water remover .
MIX-2	Waste heat boiler 1 used to recover sensible heat of off-gas	SPC	Pressure swing adsorption (PSA)
HTX-1	heat exchanger to heat mixture of natural gas and steam	MIX-5	Burner
MIX -3	Waste heat boiler 2	HTX -5	Steam boiler 2
FLA	Scrubber used to clean gas and condense water vapor in the gas.	HTX -6	Natural gas heater
HTX-2	heat exchanger 1 to preheat feed gas of water gas shift reactor	MIX-6	Steam Mixer
MIX-4	Water gas shift reactor		

Table B.5. Description of units in Figure A.5 for simulation of one-step suspension ironmaking process with SMR-H_2

Section	Unit	Description	Unit	Description
H_2 Making	MIX -1	SMR feed gas -stem mixer	SPC-2	Pressure swing adsorption (PSA)
	HTX-1	Natural gas reformer	MIX -2	H_2 Mixer
	HTG-1	Steam boiler 1	MIX-4	Burner
	MIX -2	Water gas shift reator	HTX -3	Air heater
	HTG-2	Steam boiler 2	HTX -4	Steam and natural gas heater
	MIX-3	Steam mixer	HTX -5	Natural gas heater
	HTX -2	Hot water boiler	HTX -6	Steam boiler 3
	SPC-1	Water remover .	MIX-5	Steam mixer
Iron Making	SPP-1	Ironmaking reactor .	GSC	Off-gas compressor
	HTG-3	H_2 heater	SPP-2	Water remover .
	MIX-6	Waste heat boiler (WHB)	SPC-3	Pressure Swing Adsorption (PSA)
	FLA	Scrubber used to clean gas and condense water vapor in the gas.		

Table B.6. Description of units in Figure A.6 for simulation of one-step suspension ironmaking process with SMR-syngas

Section	Unit	Description	Unit	Description
Syngas Making	MIX -1	SMR feed gas -stem mixer	HTX -3	Air heater
	HTX-1	Natural gas reformer	HTX -4	Steam and natural gas heater
	HTG-1	Steam boiler 1	HTX -5	Natural gas heater
	HTX -2	Hot water boiler	HTX -6	Steam boiler 2
	SPC-1	Water remover .	MIX-3	Steam mixer
	MIX-2	Syngas and recycle H_2 mixer		
Iron Making	MIX-4	Burner	FLA	Scrubber used to clean gas and condense water vapor in the gas.
	SPP-1	Ironmaking reactor .	GSC	Off-gas compressor
	HTG-2	Syngas and recycle H_2 heater	SPP-2	Water remover .
	MIX-5	Waste heat boiler (WHB)	SPC-2	Pressure Swing Adsorption (PSA)

APPENDIX C

DESCRIPTION OF STREAMS IN SIMULATION

BLOCK DIAGRAMS

Table C.1. Description of streams in Figure A.1 for simulation of one-step suspension ironmaking process with pure H_2

Stream Number	**Stream Name**	**Stream Temperature** (˚C)	**Stream Material** (Mt/Hr)	**Stream Energy** (GJ/Hr)
1	Iron ore concentrate	25	203.2	
2	Flux	25	7.6	
3	O_2	25	62.8	
4	Fresh H_2	25	14.5	
5	Preheated H_2	900	49.6	531.0
6	Molten iron	1500	135.7	172.0
7	Molten slag	1500	22.9	40.0
8	Fe making reactor off-gas	1500	164.7	1036.0
9	off-gas	718	164.7	455.0
10	off-gas	90	164.7	40.0
11	Cooling H_2O	25	2708.9	
12	Slurry	50	2817.1	294.0
13	off-gas	50	56.5	10.0
14	Condensed H_2O	30	21.4	
15	Recycle H_2	30	35.1	2.0

Table C.2. Description of streams in Figure A.2 for simulation of two-step suspension ironmaking process with pure H_2

Stream Number	**Stream Name**	**Stream Temperature** (˚C)	**Stream Material** (Mt/Hr)	**Stream Energy** (GJ/Hr)
1	Iron ore concentrate	25	203.2	
2	Flux	25	7.6	
3	Fresh H_2	25	12.0	
4	O_2	25	43.3	
5	Wustite	900	197.4	138.0
6	Preheated H_2	750	34.6	310.0
7	Molten iron	1500	135.7	172.0
8	Molten Slag	1500	22.9	40.0
9	Off-gas	1500	116.7	734.0
10	Feed gas of Reactor 2	1319	116.7	635.0
11	Off-gas of reactor two	900	130.1	420.0
12	WHB inlet gas	227	130.1	90.0
13	WHB outlet gas	90	130.1	29.0
14	Cooling Water	25	2,314.0	
15	Slurry	50	2,407.9	251.0
16	Off-gas	50	36.3	7.0
17	Condensed H_2O	30	21.4	
18	Recycle H_2	30	35.1	1.0

Table C.3. Description of streams in Figure A.3 for simulation of one-step reformerless suspension ironmaking process with natural gas

Stream Number	**Stream Name**	**Stream Temperature** (˚C)	**Stream Material** (Mt/Hr)	**Stream Energy** (GJ/Hr)
1	Iron ore concentrate	25	203.2	
2	Flux	25	7.6	
3	O_2	25	108.5	
4	Natural gas	380	50.6	49.1
5	Recycle H_2	30	22.5	1.6
6	Steam+H_2	144	73.0	50.7
7	Preheated H_2+Steam	900	73.0	447.5
8	Molten iron	1500	135.6	171.7
9	Molten slag	1500	22.9	39.6
10	Fe making reactor off-gas	1500	234.0	1034.9
11	Off-gas	896	234.0	583.9
12	Fresh Ngas	25	50.6	0.9
13	Preheated Ngas	380	50.6	49.1
14	WHB in -gas	787	233.8	506.3
15	WHB off-gas	90	233.8	40.6
16	Cooling H_2O	25	2854.8	
17	Slurry	50	2969.0	309.8
18	Off-gas	50	119.4	10.3
19	WGS steam	300	125.7	66.2
20	Hot WGS steam	345	245.1	212.3
21	WGS off-gas	450	245.0	290.5
22	Hot water	220	65.3	54.8
23	Steam	300	65.3	34.4
24	Off-gas	250	245.1	151.2
25	Fresh H_2O	25	358.9	
26	Hot water	220	453.6	380.3
27	Off-gas	30	245.1	4.4
28	Condensed H_2O	30	94.8	2.0
29	PSA feed gas	30	150.4	2.4
30	Recycle H_2	30	22.5	1.6
31	PSA tail gas	30	127.9	0.8
32	Air	25	154.9	
33	Combustion gas	1598	279.9	540.5
34	Hot water	220	141.1	117.5
35	Steam	300	141.1	73.7
36	Steam	300	205.5	108.1
37	Off-gas	753	282.8	241.9
38	Off-gas	300	282.8	90.1

Table C.4. Descriptions of streams in Figure A.4 for simulation of two-step reformerless suspension ironmaking process with natural gas

Stream Number	**Stream Name**	**Stream Temperature** (˚C)	**Stream Material** (Mt/Hr)	**Stream Energy** (GJ/Hr)
1	Iron ore concentrate	25	203.2	
2	Flux	25	7.6	
3	Wustite	900	197.4	138.5
4	O_2	25	79.6	
5	Natural gas	380	40.3	39.1
6	Recycle H_2	30	14.8	1.1
7	Steam+H_2	160	55.0	40.1
8	Preheated H_2+Steam	900	55.0	255.2
9	Molten iron	1500	135.9	172.0
10	Molten slag	1500	22.6	39.1
11	Fe making reactor off-gas	1500	173.5	744.8
12	Feed gas	1284	173.5	625.8
13	Off-gas	900	186.9	431.4
14	WHB2 in-gas	431	186.9	192.8
15	WHB2 off-gas	90	186.9	29.8
16	Cooling H_2O	25	2160.1	
17	Slurry	50	2246.9	234.5
18	Off-gas	50	100.1	7.5
19	WGS steam	300	88.2	46.5
20	Hot WGS steam	368	188.4	162.8
21	WGS off-gas	450	188.4	206.6
22	Hot water	220	46.5	39.0
23	Off-gas	250	188.4	107.5
24	Steam	300	46.5	24.5
25	Fresh H_2O	25	262.9	
26	Condensed H_2O	30	71.4	1.5
27	Hot water	220	334.3	280.2
28	Off-gas	30	188.4	3.2
29	PSA feed gas	30	117.0	1.7
30	Recycle H_2	30	14.8	1.1
31	PSA tail gas	30	102.2	0.6
32	Air	25	103.0	
33	Combustion gas	1507	205.3	357.7
34	Hot water	220	61.8	51.8
35	Off-gas	1000	205.3	235.9
36	Steam	300	61.8	32.5
37	Steam	300	108.3	57.0
38	Fresh Ngas	25	40.3	0.7
39	Preheated Ngas	380	40.3	39.1
40	Off-gas	796.5	205.3	184.7
41	Off-gas	300	205.3	63.9

Table C.5. Description of streams in Figure A.5 for simulation of one-step suspension ironmaking process with SMR-H_2

Section	**Stream Number**	**Stream Name**	**Stream Temperature** (˚C)	**Stream Material** (Mt/Hr)	**Stream Energy** (GJ/Hr)
H_2 Making	1	Hot Natural gas	380	49.2	47.8
	2	Steam	300	157.5	82.9
	3	SMR feed gas	600	206.7	271.7
	4	Natural gas for burner	380	4.8	4.7
	5	Hot air	800	431.1	367.9
	6	Combustion gas	2353	551.2	1711.0
	7	Combustion gas	1508	551.3	1044.5
	8	Air	25	431.1	
	9	Preheated air	800	431.1	367.9
	10	Combustion gas	1011	551.2	676.6
	11	Preheated Natural gas	380	49.2	47.8
	12	SMR Steam	300	157.5	82.9
	13	Preheated Natural gas and steam	600	206.7	271.7
	14	Combustion gas	814.4	551.6	535.6
	15	SMR natural gas	25	49.2	843.0
	16	Combustion natural gas	25	4.8	
	17	Hot Natural gas	380	54.0	52.5
	18	Combustion gas	741	551.3	
	19	Hot water added to steam boiler 3	220	74.4	62.4
	20	Steam	300	74.4	39.2
	21	Combustion gas	513	551.3	325,4
	22	Combustion gas	300	551.3	180.7
	23	Reformed gas	850	206.7	470.1
	24	Hot water	220	129.6	108.6

Table C.5 Continued

H_2 Making	25	Steam	300	129.6	68.2
	26	Reformed gas	382	206.7	193.9
	27	Reformed gas	450	206.7	235.9
	28	Hot water added to steam boiler 2	220	53.5	44.8
	29	Steam	300	53.5	28.1
	30	Steam	300	183	96.3
	31	Reformed gas	250	206.7	121.9
	32	Fresh water add to hot water boiler	25	291.7	
	33	Hot water	220	369.4	309.7
	34	Mixed gas	30	206.7	3.7
	35	Condensed H_2O	30	77.7	1.6
	36	PSA feed gas	30	129.0	2.0
	37	H_2 from SMR	30	16.7	1.2
	38	Tail gas from SMR	30	112.4	0.9
	39	Mixed H_2	30	37.0	2.6
	40	Feed H_2	30	37.0	2.6
	41	Preheated Feed H_2	900	37.0	477.8
Iron making	42	Iron ore concentrate	25	203.2	
	43	Flux	25	7.6	
	44	O_2	25	59.9	
	45	Molten iron	1500	135.9	172.0
	46	Molten slag	1500	22.6	39.1
	47	Ironmaking off-gas	1500	149.3	939.1
	48	Ironmaking off-gas	725	149.3	416.8
	49	Scrubber feed gas	90	149.3	36.4
	50	Cooling H_2O	25	2455.1	
	51	Slurry	50	2553.2	266.4
	52	Scrubber off- gas	50	51.2	9.5
	53	Wet H_2	30	51.2	2.2
	54	Condensed H_2O	30	27.9	0.6
	55	H_2 with saturated water	30	23.4	1.6
	56	Recycle H_2	30	20.3	1.5
	57	Emitted gas from ironmaking	30	3.0	0.2

Table C.6. Description of streams in Figure A.6 for simulation of one-step suspension ironmaking process with SMR-syngas

Section	Stream Number	Stream Name	Stream Temperature (˚C)	Stream Material (Mt/Hr)	Stream Energy (GJ/Hr)
Syngas Making	1	Hot Natural gas	380	51.1	49.6
	2	SMR Steam	300	163.3	86
	3	SMR feed gas	600	214.4	281.9
	4	Natural gas for burner	380	5.9	5.7
	5	Hot air	800	398	339.7
	6	Combustion gas	2714	502.5	1731.9
	7	Combustion gas	1709	502.5	1040.1
	8	Air	25	398	
	9	Preheated air	800	398	339.7
	10	Combustion gas	1185	502.5	700.5
	11	Preheated Natural gas	380	51.1	49.6
	12	SMR Steam	300	163.4	86
	13	Preheated Natural gas and steam	600	214.5	281.9
	14	Combustion gas	953	502.5	554.2
	15	SMR natural gas	25	51.1	874.6
	16	Combustion natural gas	25	5.9	0.1
	17	Hot Natural gas	380	57	55.3
	18	Combustion gas	865	502.5	499.8
	19	Hot water added to steam boiler 2	220	96.7	81
	20	Steam added	300	96.7	50.9
	21	Combustion gas	527	502.5	293.8
	22	Emitted combustion gas	300	502.5	158.8
	23	Reformed gas	850	214.5	487.7
	24	Hot water	220	170.5	142.9
	25	Steam	300	170.5	89.7

Table C.6 Continued

Syngas Making	26	Reformed gas	250	214.5	124.4
	27	Fresh water add to hot water boiler 1	25	336.9	
	28	hot water produced	220	436.6	366.0
	29	Reformed gas	30	214.4	4.0
	30	Syngas produced	30	114.8	1.9
	31	Condensed H_2O	30	99.7	2.1
Ironmaking	32	Ironmaking feed-gas	30	138.6	3.6
	33	Hot ironmaking feed gas	900	138.6	641.9
	34	Iorn ore concentrate	25	203.2	
	35	Flux	25	7.6	
	36	O_2	25	78.3	
	37	Molten iron	1500	135.9	172.0
	38	Molten slag	1500	22.6	39.1
	39	Ironmaking off-gas	1500	269.2	1253.2
	40	Ironmaking off-gas	716	269.2	552
	41	Scrubber feed gas	90	269.2	49.1
	42	Cooling H_2O	25	2724.1	
	43	Slurry	50	2830.6	295.4
	44	Scrubber off- gas	50	162.7	14.0
	45	Wet H_2	30	162.7	3.3
	46	Condensed H_2O	30	40.2	0.8
	47	H_2 with saturated water	30	122.4	2.4
	48	Recycle H_2	30	23.8	1.7
	49	Emitted gas from ironmaking	30	98.7	0.7

APPENDIX D

REACTIONS TAKING PLACE IN REACTORS

Table D.1. Reactions taking place in simulated one-step and two-step suspension ironmaking processes with pure H_2 process.

Description	**Reaction**	**Location**	**Reaction Extent**
Fuel combustion	$2H_2 + O_2 = 2H_2O$	Ironmaking Reactor	1
Reduction of iron oxide	$Fe_3O_4 + H_2 = 3FeO + H_2O$	Ironmaking Reactor in one-step. Pre-reduce reactor in two step reactor.	1
	$FeO + H_2 = Fe + H_2O$	Ironmaking reactor	0.967-0.990 varying with temperature and H_2 drving force
Slag forming	$CaO(s) = CaO(l)$	Ironmaking Reactor	1
	$SiO_2(s) = SiO_2(l)$	Ironmaking Reactor	1
	$Al_2O_3(s) = Al_2O_3(l)$	Ironmaking Reactor	1
	$MgO(s) = MgO(l)$	Ironmaking Reactor	1

Table D.2. Reactions taking place in simulated one-step and two-step reformerless suspension ironmaking processes with natural gas

Description	Reaction	Location	Reaction Extent
Fuel combustion	$2C_2H_6 + 7O_2 = 6H_2O + 4CO_2$	Ironmaking reactor	1
	$CH_4 + 2O_2 = 2H_2O + CO_2$	Ironmaking reactor	1
	$2H_2 + O_2 = 2H_2O$	Burner	1
	$2CO + O_2 = 2CO_2$	Burner	1
Methane reforming by water vapor	$CH_4 + H_2O = 3H_2 + CO$	Ironmaking reactor	Equilibrium at the ironmaking reactor temperature
Reduction of iron oxide by hydrogen	$Fe_3O_4 + H_2 = 3FeO + H_2O$	Ironmaking reactor in one step process but pre-reduce reactor in two step process	1
	$FeO + H_2 = Fe + H_2O$	Ironmaking reactor	0.967-0.990
Reverse water gas shift reaction	$CO_2 + H_2 = CO + H_2O$	Ironmaking reactor	Equilibrium at the ironmaking reactor temperature. 900^oC in the prereduction reactor.
Slag forming	$CaO(s) = CaO(l)$	Ironmaking reactor	1
	$SiO_2(s) = SiO_2(l)$	Ironmaking reactor	1
	$Al_2O_3(s) = Al_2O_3(l)$	Ironmaking reactor	1
	$MgO(s) = MgO(l)$	Ironmaking reactor	1
Water gas shift reaction	$CO + H_2O = CO_2 + H_2$	Water gas shift reactor	Equilibrium at 450^oC
Steam generation	$H_2O(l) = H_2O(g)$	Steam boilers	1
Water condensation	$H_2O(g) = H_2O(l)$	Scrubber, Boiler feed water (BFW)	Saturation at 30^oC, 1800 kPa in BFW. Saturated at 50 ˚C, at 800 kPa in scrubber.

Table D.3. Reactions taking place in simulated one-step suspension ironmaking processes with SMR-H_2

Description	Reaction	Location	Reaction Extent
Fuel combustion	$2C_2H_6 + 7O_2 = 4CO_2 + 6H_2O$	Burner	1
	$CH_4 + 2O_2 = CO_2 + 2H_2O$	Burner	1
	$2H_2 + O_2 = 2H_2O$	Burner and ironmaking reactor	1
	$2CO + O_2 = 2CO_2$	Burner	1
Reduction of iron oxide	$Fe_3O_4 + H_2 = 3FeO + H_2O$	Ironmaking reactor	1
	$FeO + H_2 = Fe + H_2O$	Ironmaking reactor	0.967-0.990
Slag forming	$CaO(s) = CaO(l)$	Ironmaking reactor	1
	$SiO_2(s) = SiO_2(l)$		1
	$Al_2O_3(s) = Al_2O_3(l)$		1
	$MgO(s) = MgO(l)$		1
Steam-methane reforming	$CH_4 + H_2O = 3H_2 + CO$	Reformer	0.825 (to make CH_4 in the reformed gas 3%)
	$C_2H_6 + 2H_2O = 2CO + 5H_2$		1
	$CO + H_2O = CO_2 + H_2$		Equilibrium at 850°C
Steam generation	$H_2O(l) = H_2O(g)$	Steam boilers	1
Water gas shift reaction	$CO + H_2O = CO_2 + H_2$	Water gas shift reactor	Equilibrium at 450°C
Condensation	$H_2O(g) = H_2O(l)$	Scrubber and Boiler feed water heater	Saturation at 30°C, 1800 kPa in BFW. Saturated at 50 ˚C, at 800 kPa in scrubber.

Table D.4. Reactions taking place in simulated one-step suspension ironmaking processes with SMR-syngas

Description	Reaction	Location	Reaction Extent
Fuel combustion	$2C_2H_6 + 7O_2 = 4CO_2 + 6H_2O$	Burner	1
	$CH_4 + 2O_2 = CO_2 + 2H_2O$	Burner and ironmaking reactor	1
	$2H_2 + O_2 = 2H_2O$	Burner and ironmaking reactor	1
	$2CO + O_2 = 2CO_2$	Burner and ironmaking reactor	1
Reduction of iron oxide	$Fe_3O_4 + H_2 = 3FeO + H_2O$	Ironmaking reactor	1
	$FeO + H_2 = Fe + H_2O$		0.967-0.990
Slag forming	$CaO(s) = CaO(l)$	Ironmaking reactor	1
	$SiO_2(s) = SiO_2(l)$		1
	$Al_2O_3(s) = Al_2O_3(l)$		1
	$MgO(s) = MgO(l)$		1
Steam generation	$H_2O(l) = H_2O(g)$	Steam boilers	1
Reverse water gas shift reaction	$CO_2 + H_2 = CO + H_2O$	Ironmaking reactor	Equilibrium at the reactor operating temperature
Condensation	$H_2O(g) = H_2O(l)$	Scrubber and Boiler feed water heater	Saturation at 30^{o}C, 1800 kPa in BFW. Saturated at 50 ˚C, at 800 kPa in scrubber.

APPENDIX E

SENSITIVITY ANALYSIS OF ECONOMICS DIAGRAMS

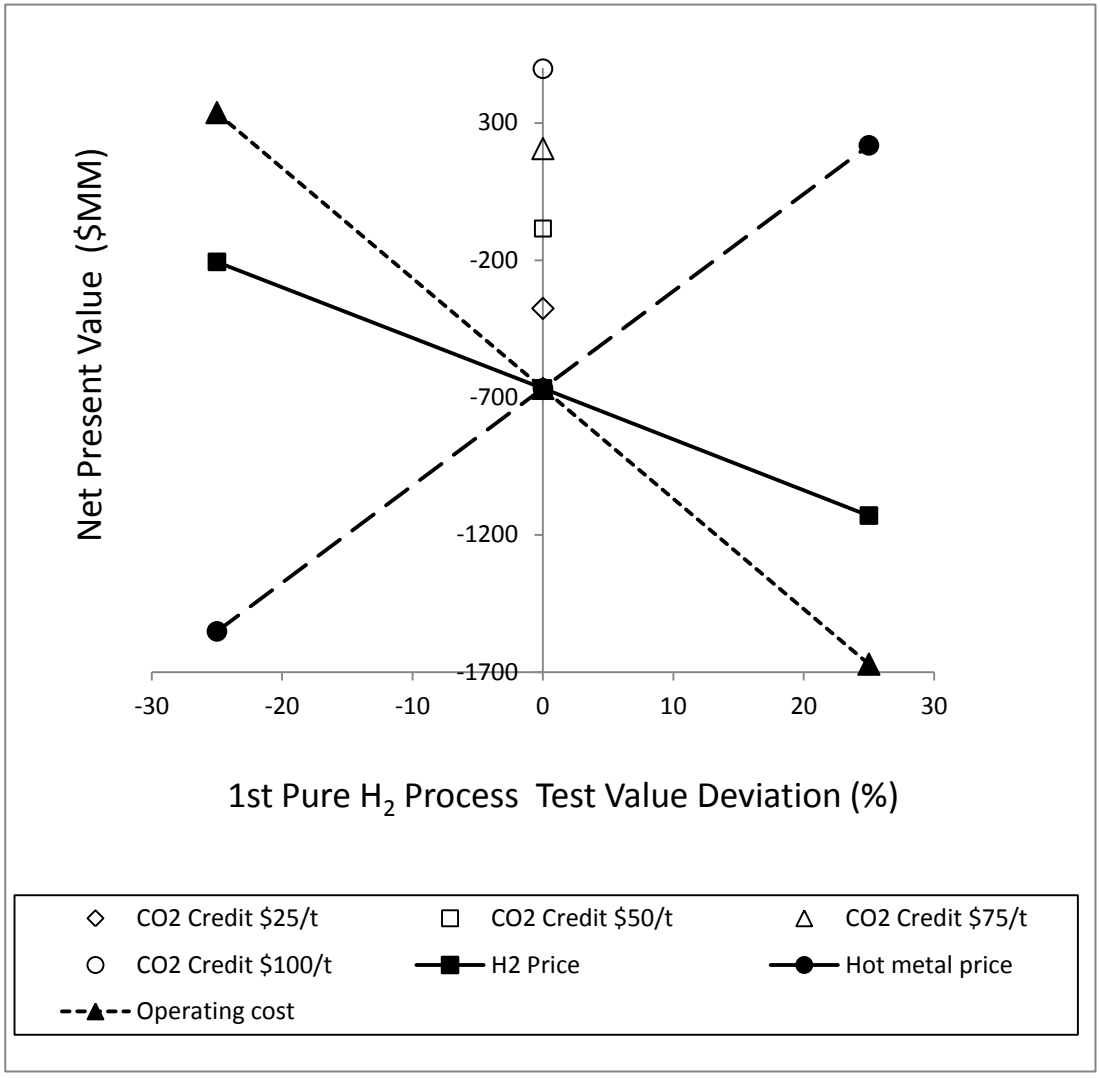

Figure E.1. Sensitivity analysis of economics for one-step suspension ironmaking process with pure H_2

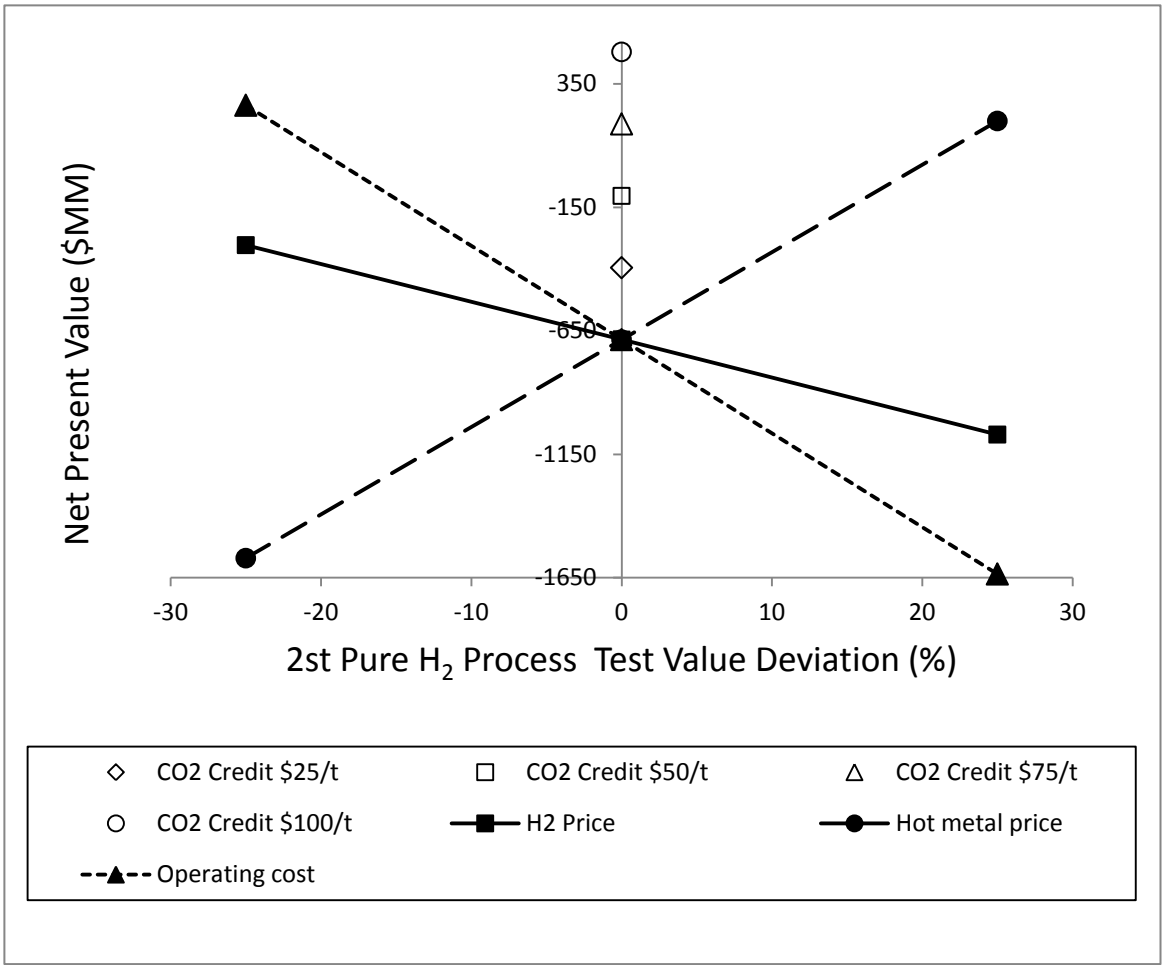

Figure E.2. Sensitivity analysis of economics for two-step suspension ironmaking process with pure H_2

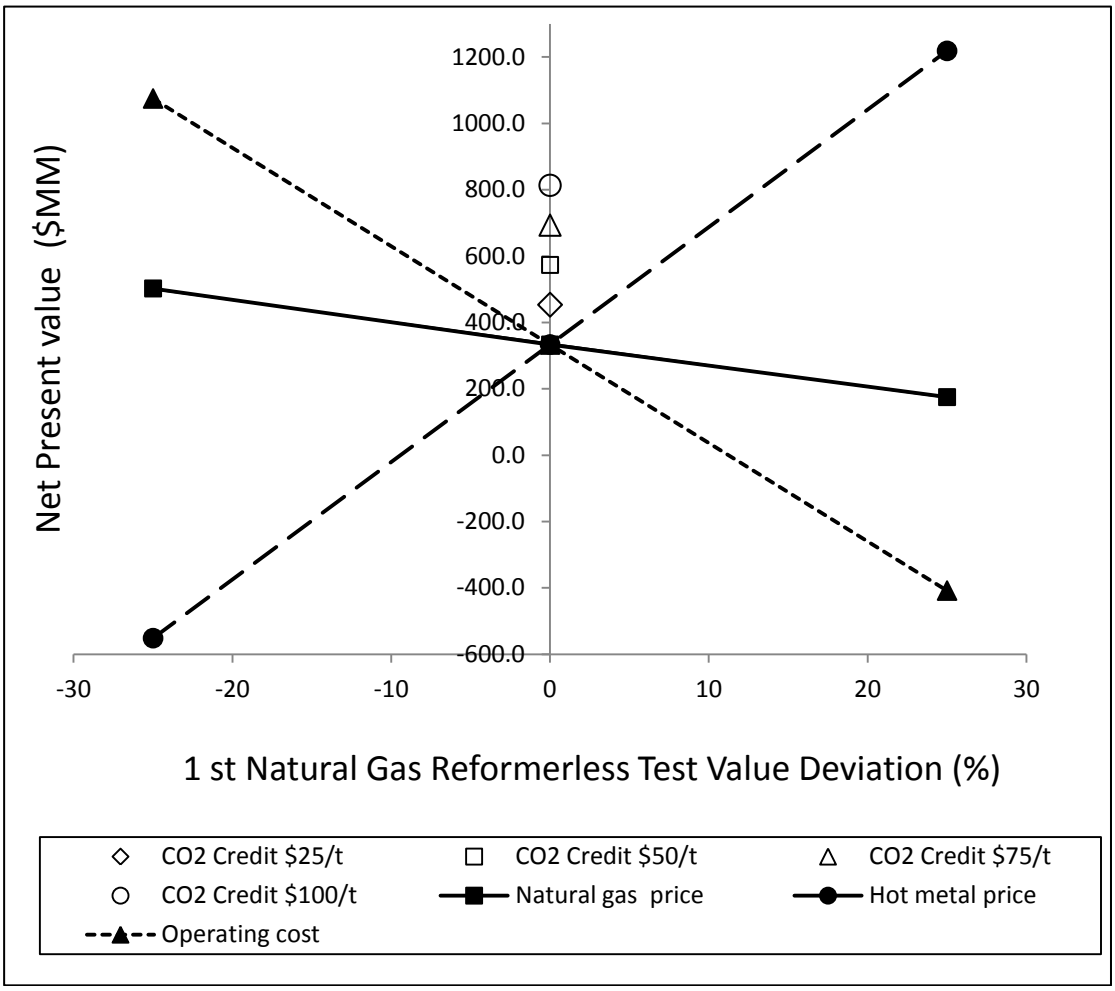

Figure E.3. Sensitivity analysis of economics for one-step reformerless suspension ironmaking process with natural gas

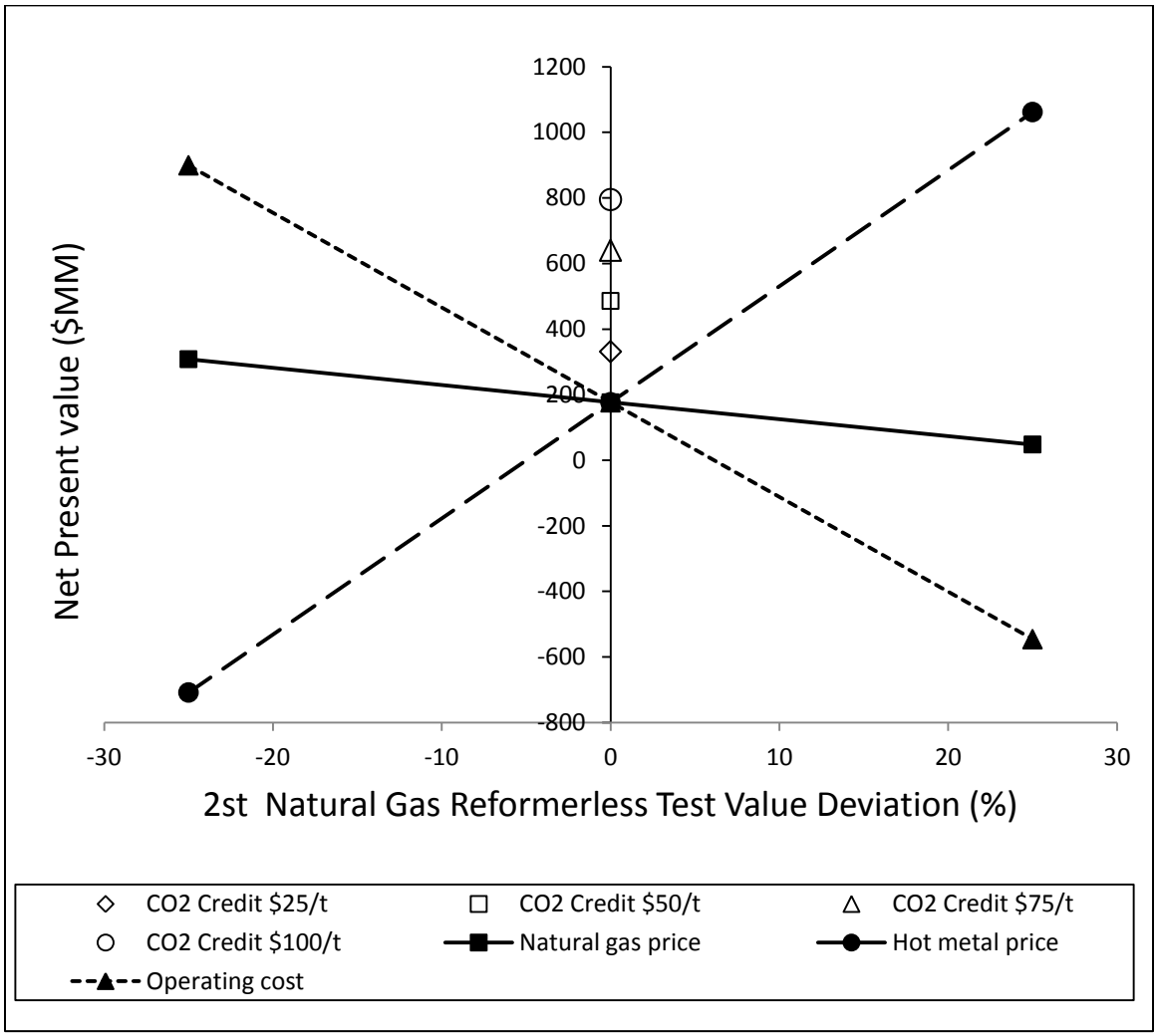

Figure E.4. Sensitivity analysis of economics for two-step reformerless suspension ironmaking process with natural gas

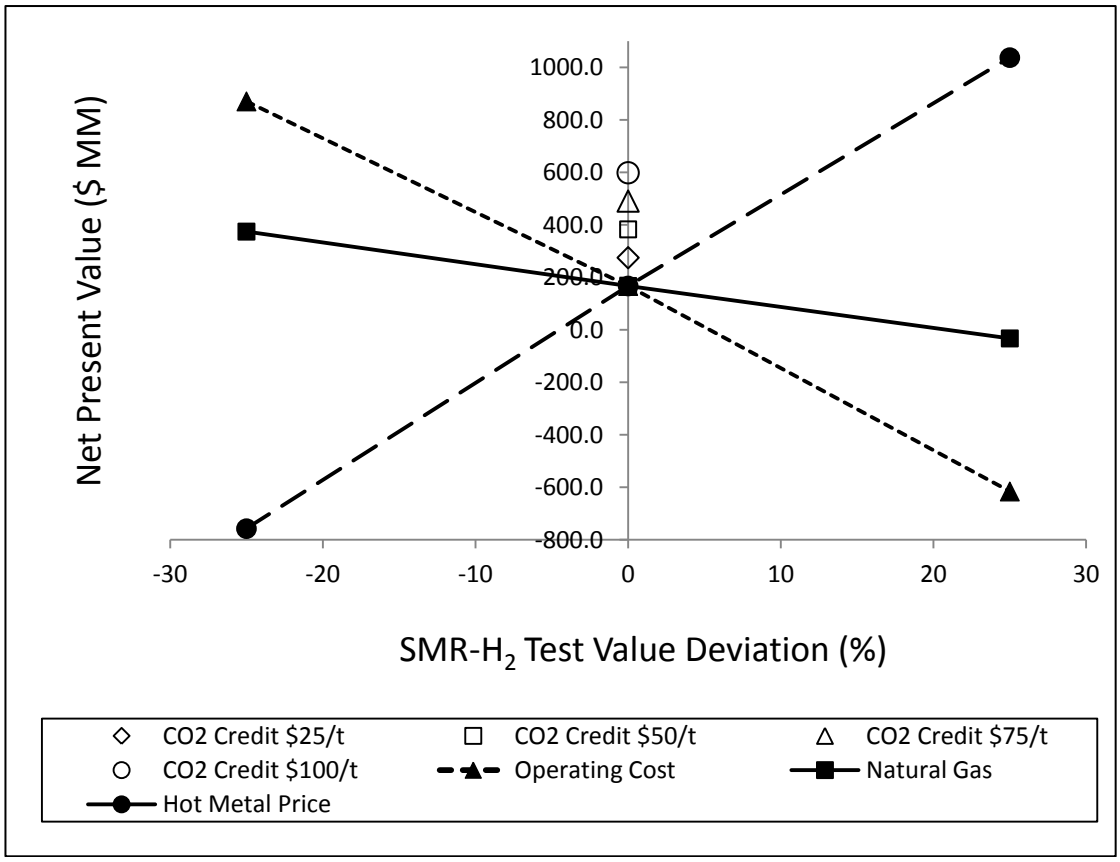

Figure E.5. Sensitivity analysis of economics for one-step suspension ironmaking process with SMR-H_2

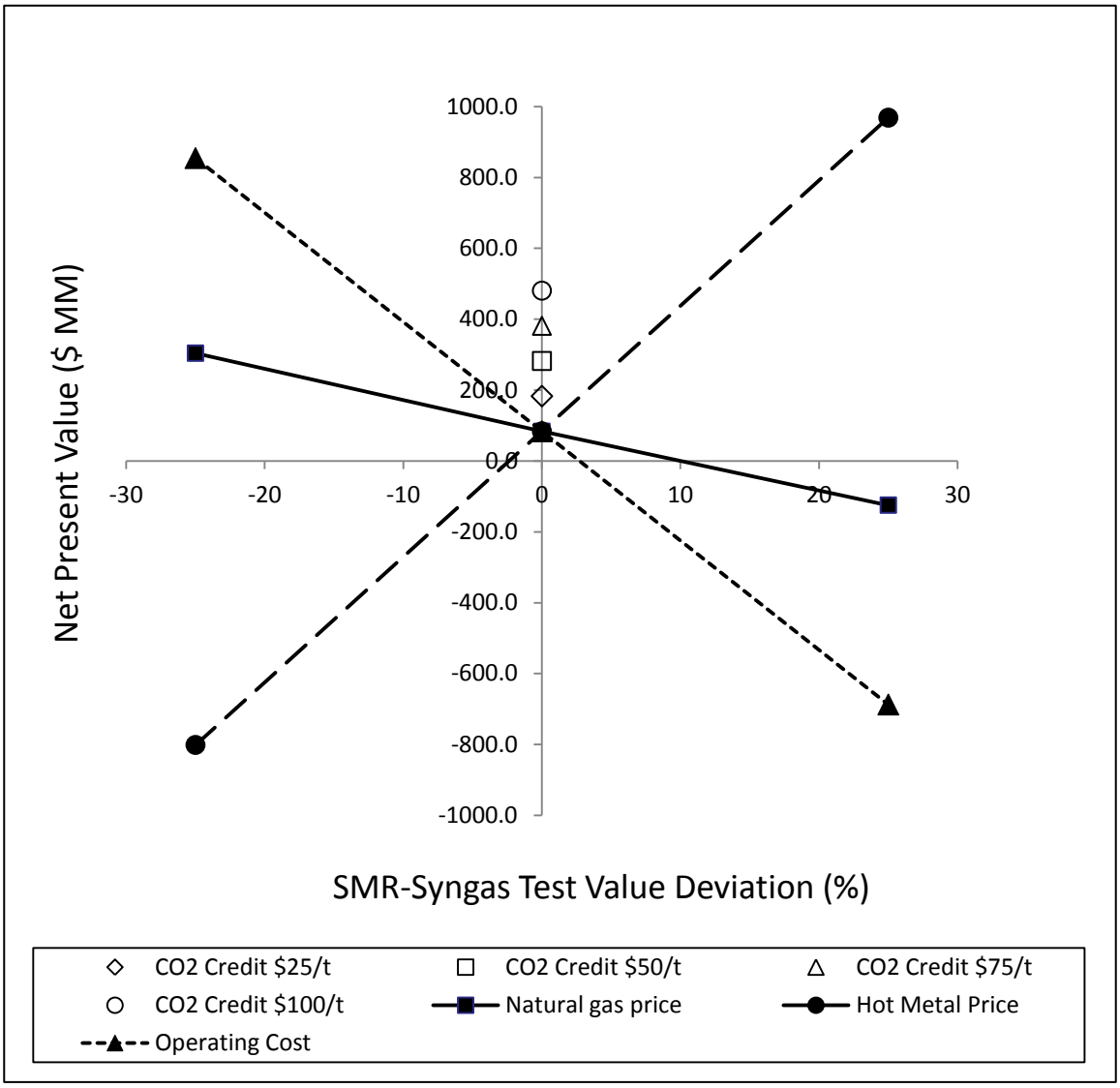

Figure E.6. Sensitivity analysis of economics for one-step suspension ironmaking process with SMR-syngas

REFERENCES

[1] S. Gupta and V. Sahajwalla, "The scope for fuel rate reduction in ironmaking," in *Technical Note 16*, J. Gurgess, Ed. The University of New South Wales, January. 2005.

[2] Y. Zhou, H. Qian, Y. Zhang, Z. Li, J. Fan, "Advantages and disadvantages and its research direction of present ironmaking processes," *Iron and steel,* vol. 44, no.2, pp. 1-10, Februay. 2009.

[3] M. Komatina and H. W. Gudenau, "The sticking problem during direct reduction of fine iron ore in the fluidized bed," *Metalurgija-Journal of Metallurgy,* pp. 309-328, November. 2004.

[4] F. Grobler and R. C. Minnitt, "The increasing role of direct reduced iron in global steelmaking," *The Journal of The South African Institute of Mining and Metallurgy,* pp. 111-116, March / April, 1999.

[5] R. J. Fruehan, "Future iron and steelmaking in the USA," *Scandinavian Journal of Metallurgy,* vol. 28, pp. 77-85, 1999.

[6] J. D. Beer, W. Warrell and K. Blok, "Future technologies for energy - efficient iron and steel making," *Annual Review Energy Environment,* vol. 23, pp. 123-205, 1998.

[7] H. Y. Sohn, "Suspension ironmaking technology with greatly reduced energy requirement and CO_2 emissions," *Steel Times International,* pp. 68-72, 2007, May/June, 2007.

[8] H. Y. Sohn, "Novel ironmaking technology with greatly reduced CO_2 emission and energy consumption," presented at the 2008 Scrap Substitutes and Alternative Ironmaking V, AIST, Baltimore, USA, 2008.

[9] H. Y. Sohn, M. E. Choi, Y. Zhang and J. E. Ramos, "Suspension ironmaking technology with greatly reduced CO_2 emission and energy requirement," in *Energy Technology Perspectives: Carbon Dioxide Reduction and Production from Alternative Sources, TMS*, Warrendale, PA, 2009, pp. 93-101.

[10] H. Y. Sohn, M. E. Choi, Y. Zhang and J. E. Ramos, "Suspension reduction technology for ironmaking with low CO_2 emission and energy requirement," *Iron & Steel Technology,* vol. 6, no.8, pp. 158 -165, 2009.

[11] H. Y. Sohn, M. E. Choi and Keynote Lecture, "Development of a novel gas-suspension ironmaking technology with greatly reduced consumption and CO_2 emissions," in *Supplemental Proceedings: Vol. 1 Materials Processing and Properties, International Symposium on High-Temperature Metallurgical Processing,* 139th TMS Annual.

Meeting, Seattle, WA, 2010, pp. 347-354.

[12] H. Kimura, S. Liu, M. S. Moats and H. Y. Sohn, "Process simulation for a novel green ironmaking technology with greatly reduced CO_2 and energy consumption," *SME Annual Meeting,* Phoenix, AZ, 2010.

[13] H. K. Pinegar, M. S. Moats and H. Y. Sohn, "Flow sheet development, process simulation and economic feasibility analysis for a novel suspension ironmaking technology based on natural gas: part I. flow sheet and simulation for ironmaking with reformerless natural gas," *Ironmaking steelmaking,* to be published.

[14] H. K. Pinegar, M. S. Moats and H. Y. Sohn, "Flow sheet development, process simulation and economic feasibility analysis for a novel suspension ironmaking technology based on natural gas: part II. flow sheet and simulation for ironmaking combined with steam-methane reforming," *Ironmaking steelmaking,* to be published.

[15] H. K. Pinegar, M. S. Moats and H. Y. Sohn, "Process simulation and economic feasibility analysis for a hydrogen-based novel suspension ironmaking technology," *Steel Research International*, vol. 82, no, 8, 2011.

[16] H. K. Pinegar, M. S. Moats and H. Y. Sohn, "Flow sheet development, process simulation and economic feasibility analysis for a novel suspension ironmaking technology based on natural gas: part III. economic feasibility analysis," *Ironmaking steelmaking,* to be published.

[17] H. Kimura, "Material and energy flow simulation and economic analysis for a novel suspension ironmaking technology," M.S. Thesis, Metallurgical Engineering, Universtiy of Utah, Salt Lake City, UT, 2010.

[18] H. M. Henao and K. Itagaki, "Activity and activity coefficient of iron oxides in the liquid FeO-Fe_2O_3-CaO-SiO_2 slag systems at intermediate oxygen partial pressures," *Metallurgical and Materials Transactions, B,* vol. 38B, pp. 769-780, 2007.

[19] M. Timucin and A. E. Morris, "Phase equilibria and thermodynamic studies in the system CaO-FeO-Fe_2O_3-SiO_2," *Metallurgical Transaction,* vol. 1, pp. 3193-3201, November. 1970.

[20] T. Ogura, R. Fujiwara, R. Mochizuki, Y. Kawamoto, T. Oishi and M. Iwase," Activity determinator for the automatic measurments of the chemical potentials of FeO in metallurgical slags," *Metallurgical and Materials Transactions, B,* vol. 23, pp. 459-466, 1992.

[21] H. Ohta and H. Suito, "Activities of SiO_2 and Al_2O_3 and activity coefficients of Fe_tO and MnO in CaO-SiO_2-Al_2O_3-MgO slags," *Metallurgical and Materials Transactions. B,* vol. 29B, pp. 119-129, 1998.

[22] H. Fujiwara, "Thermodynamics of iron oxide in Fe_xO-dilute CaO+Al_2O_3+SiO_2+Fe_xO slags at 1873K," *Steel Research,* vol. 71, pp. 53-59, 2000.

[23] P. Fredriksson and S. Seetharaman, "Thermodynamic activities of "FeO" in some binary "FeO"-containing slags," *Steel Reserch Internationl,* vol. 75, p. 240, 2004.

[24] P. Fredriksson and S. Seetharaman, "Thermodynamic activities of "FeO" in some

ternary "FeO"-containing slags," *Steel Research International,* vol. 75, pp. 357-365, 2004.

[25] Q. Lu, L. S. Zao, C. Wang and S. H. Zhang, "Activities of FeO in CaO-SiO_2-Al_2O_3-MgO-FeO slags," *J. Shanghai University,* vol. 12, pp. 466-470, 2008.

[26] S. Ban-Ya, "Mathematical expression of slag - metal reactions in steelmaking process by quadratic formalism based on the regular solution model" *ISIJ. International,* vol. 33, pp. 2-11, 1993.

[27] J. M. Park and K. K. Lee, "Reaction equilibria between liquid iron and CaO-Al_2O_3-$MgO_{sat.}$-SiO_2-MnO-P_2O_5 slag," presented in 1996 Steelmaking Conferen*ce*, 1996, pp. 165-171.

[28] D. P. Tao, "Prediction of activities of three components in the ternary molten slag CaO-FeO-SiO_2 by the molecular interaction volume model," *Metallurgical and Materials Transactions. B,* vol. 37B, pp. 1091-1097, 2006.

[29] M. Meraikib, "Effect of direct reduced iron on oxygen distribution between slag and bath in electric arc furnaces," *Steel Research. International,* vol. 79, pp. 340-347, 2008.

[30] C. R. Taylor and J. Chipman, "Equilibria of liquid iron and simple basic and acid slags in rotating induction furnace," presented at *the Cleveland Meeting,* 1942.

[31] Metsim, "The remier process simulator for window," February, 2011, http://www.metsim.com

[32] Average pig iron price, "Basic pig iron foundry Midwest (USD/MT) in Chicago iron tables," September 2010, http://www.metalprices.com/freesite/metals/fe chicago.asp#Tables

[33] M. S. Peters and K. D. Timmerhaus, *Plant Design and Economics for Chemical Engineers,* 4th Ed., McGraw-Hill, NY, 1991, pp. 163-169.

[34] "CEPCI," September 2010, http://www.scribd.com/doc/32627641/CEPCI

[35] M. M. Miller, "Lime statistics and information" in *Minerals Year Book*, *Mineral Commodity Summaries*, January 2011, p. 92-93. http://minerals.usgs.gov/minerals/pubs/commodity/lime/mcs-2011-lime.pdf